Available online at www.sciencedirect.com
ScienceDirect
Journal of Asian Earth Sciences 30 (2007) 573–590
Journal of Asian Earth Sciences
www.elsevier.com/locate/jaes

Zircon ages and Nd–Hf isotopic composition of the Zhaertai Group (Inner Mongolia): Evidence for early Proterozoic evolution of the northern North China Craton

Qiu-Li Li [a,b], Fukun Chen [a,b,*], Jing-Hui Guo [a], Xiang-Hui Li [b], Yue-Heng Yang [a], Wolfgang Siebel [c]

[a] State Key Laboratory of Lithospheric Evolution, Institute of Geology and Geophysics, Chinese Academy of Sciences, Beijing 100029, China
[b] Laboratory for Radiogenic Isotope Geochemistry, Institute of Geology and Geophysics, Chinese Academy of Sciences, Beijing 100029, China
[c] Institut für Geowissenschaften, Universität Tübingen, 72074 Tübingen, Germany

Received 6 July 2006; received in revised form 11 December 2006; accepted 19 January 2007

Abstract

The Mesoproterozoic rifting and accompanying magmatism and sedimentation in the North China Craton are interpreted to be related to the breakup of the Paleoproterozoic supercontinent Columbia. This study presents zircon ages and Nd–Hf isotopic data of the low-grade Mesoproterozoic Zhaertai Group exposed along the northern margin of the North China Craton. Sandstones of the Zhaertai Group contain detrital zircon populations of about 2500 Ma, which originated from the late Archean basement rocks underlying this group. A close match between the U–Pb ages and the T_{DM} (Hf) ages with high initial ε_{Hf} values (at 2500 Ma) for the detrital zircon grains imply a juvenile origin for protoliths of the basement rocks. Sedimentation of the Zhaertai Group likely began around 1750 Ma tentatively constrained by the formation time of an intercalated volcanic layer. The volcanic rocks have low initial ε_{Nd} values of −8.0 to −8.5 (at 1750 Ma), similar to those of contemporaneous mafic dyke swarms within the North China Craton, which have been interpreted to be related either to the breakup of the supercontinent Columbia or to the post-collisional collapse of the Trans-North China Orogen. A progressive increase of ε_{Nd} values of whole-rock samples upwards in the stratigraphic sequence likely indicates an increase of juvenile material with time probably related to the contribution of Mesoproterozoic mantle-derived rocks.

Keywords: Mesoproterozoic; North China Craton; Zhaertai Group; Detrital zircon age; Nd–Hf isotopes

1. Introduction

Geological investigations have been intensively performed in the North China Craton since the beginning of the last century and significant progress has been achieved in recent years. Nevertheless, the complex history of this craton has lead to the proposition of diverse models for the tectonic evolution (e.g., Zhai, 2004a,b; Zhao et al., 1998, 2000, 2001, 2002, 2005; Li et al., 2000, 2002; Lu et al., 2002; Kusky and Li, 2003; Kusky et al., 2001). The North China Craton was originally considered as a uniform Archean crystalline basement (e.g., Huang, 1977). Zhao et al. (1998) proposed a Paleoproterzoic orogen (termed as the Central Zone) along the central North China Craton, separating it into the Western and Eastern Blocks. Further data appear to support that at least three Paleoproterozoic orogenic belts exist within the North China Craton (Zhao et al., 2005). More complex tectonic subdivisions have been proposed by Zhang et al. (1998); Wu and Zhang (1998) and Zhai et al. (2000). For detailed accounts the reader is referred to the recent review by Zhao et al. (2005). The main points of the dispute on the tectonic evolution of the North China Craton are whether the amalgamation of the tectonic units took place in the late

* Corresponding author. Fax: +86 10 62010846.
E-mail address: fukun-chen@mail.igcas.ac.cn (F. Chen).

1367-9120/$ - see front matter © 2007 Elsevier Ltd. All rights reserved.
doi:10.1016/j.jseaes.2007.01.006

Archean (Li et al., 2000; Kusky and Li, 2003) or in the late Paleoproterozoic (Zhao et al., 1998, 1999, 2000, 2002, 2003, 2005) and which of the tectonic events recorded in the North China Craton occurred during the Paleoproterozoic (e.g., Zhai et al., 2000; Zhai, 2004a,b). A Paleoproterozoic amalgamation is primarily supported by the occurrence of high-pressure granulite-facies metamorphism at about 1800–1900 Ma (Wu and Zhang, 1998; Zhao et al., 2001, 2002; Wilde et al., 2002; Guo et al., 2002).

Numerous magmatic rocks, late Paleoproterozoic to early Mesoproterozoic in age, including rapakivi granites, anorthosites, mafic dike swarms, and volcanic rocks exposed in the North China Craton (e.g., Halls et al., 2000; Wilde et al., 2002, 2004; Peng et al., 2004, 2005), are interpreted as products related to the breakup of the Paleoproterozoic supercontinent Columbia (Peng et al., 2005; Peng, 2005). Contemporaneous sedimentation can be widely traced in different parts of the block (e.g., Ma et al., 1987). Along the northern margin of the North China Craton, several sedimentary sequences of probably Mesoproterozoic age, such as the Zhaertai and Bayan Obo Groups, are exposed. These sediments were deposited in an E–W trending marginal basin during the opening of the Paleo-Mongolia Ocean or the Langshan-Baiyun Obo rifting systems (Wang et al., 1992; Zhang et al., 1999). This study focuses on the provenance and sedimentation age of the low-grade Mesoproterozoic Zhaertai Group in order to reveal information about the pre-Mesoproterozoic evolution of the northern North China Craton. We report geochemical and Nd isotopic composition of whole-rock samples and U–Pb ages and Hf isotopic composition of detrital zircon grains from sedimentary rocks and intercalated volcanic layers.

2. Geological setting of the Zhaertai Group and samples

The North China Craton consists mainly of Archean to Paleoproterozoic rocks. To the north, it is bounded by the late Paleozoic Central Asian Orogenic Belt and to the south, it is separated from the South China block by the early Mesozoic Qinling-Dabie-Sulu ultrahigh-pressure orogenic belt (e.g., Ma and Bai, 1998; Mattauer et al., 1985; Meng and Zhang, 2000; Sengör and Natal'in, 1996). The basement rocks of the North China Craton are largely covered by late Proterozoic to Cenozoic sedimentary sequences and are intruded by Mesozoic to Cenozoic magmatic rocks (e.g., Huang, 1977; Ma and Bai, 1998). In local areas, Mesoproterozoic low-grade metamorphic to unmetamorphosed rock sequences are exposed, which are represented by the Changcheng Group (or System) and the Jixian Group (or System) in the central part of the craton, the Xiyanghe and Xiong'er Groups along the southern margin, and the Zhaertai, Bayan Obo, Bainaimiao, and Huade Groups along the northern margin (e.g., Chen and Wu, 1997). They are commonly interpreted as the sedimentary cover rocks related to Mesoproterozoic rift after cratonization of the North China Craton in the late Paleoproterozoic (e.g., Zhai, 2004a,b; Zhai and Liu, 2003; Shao et al., 2001; Lu et al., 2002; Qian, 1996; Rämä et al., 1995).

The Zhaertai Group exposed in the central part of Inner Mongolia belongs to the northern margin of the North China Craton or the Yinshan block (e.g., Zhao et al., 2005). It crops out in an E-W trending zone, approximately 600 km long in the Zhaertai Mountains (partly shown in Fig. 1C). The Zhaertai Group is commonly separated into four rock formations, from bottom to top, the Shujigou, Zenglongchang, Agulugou, and Liuhongwang Formations (Fig. 1D). Major rock types include low-grade metaconglomerates with magnetite quartzite pebbles, conglomeratic arkose quartz sandstones, quartzites, dolomites, dolomitic slates, phyllites, and carbonaceous phyllites. The Zhaertai Group is covered unconformably by the Permian Dahongshan Formation and unconformably overlies the late Archean Serertangshan Group, the latter consisting of mica quartz schists, migmatites, and granites.

Wang et al. (1992) suggested that these low-grade metamorphosed sediments formed at around 1600 Ma and were deposited along the eastern margin of a fault-bounded basin termed as the Langshan-Baiyun Obo basin. Zhang et al. (1999) argued that the Zhaertai, Bayan Obo and Bainaimiao Groups were deposited in an E–W trending marginal rift situated at the northern margin of the North China Craton during the opening of the Paleo-Mongolia Ocean. Regional geological maps of the Inner Mongolia autonomous region depict the Zhaertai Group as part of the Changchengian system. This correlation is based on two stromatolithic horizons. The lower one occurs in the lower part of the Zenglongchan Formation, characterized by the Eucapsiphora-*Colonnella* assemblage, whereas the upper one is located in the upper part of Agulugou Formation, dominated by the *Conophyton-Tabuloconigera* assemblage. These two horizons may be correlated with stromatolites of Changchengian age in the Yanshan area of the North China Craton. The Shujigou Formation of the Zhaertai Group contains intercalated basaltic volcanic layers with vesicle and amygdaloidal structures, indicating formation at the time of sedimentation.

Seven quartz sandstone samples, representing the major sedimentary components of the Shujigou Formation, were systemically collected from bottom to top. Five pelitic rocks were sampled from the Agulugou Formation. Seven samples of volcanic rock and three migmatitic granite samples underlying the Shujigou Formation were also collected. Rock types and sample localities are given in Table 1.

3. Analytical methods

3.1. Geochemical analysis

Major and trace elements were analyzed at the Institute of Geology and Geophysics, Chinese Academy of Sciences (IGG CAS). Major elements were determined by X-ray fluorescence spectrometry with analytical uncertainties

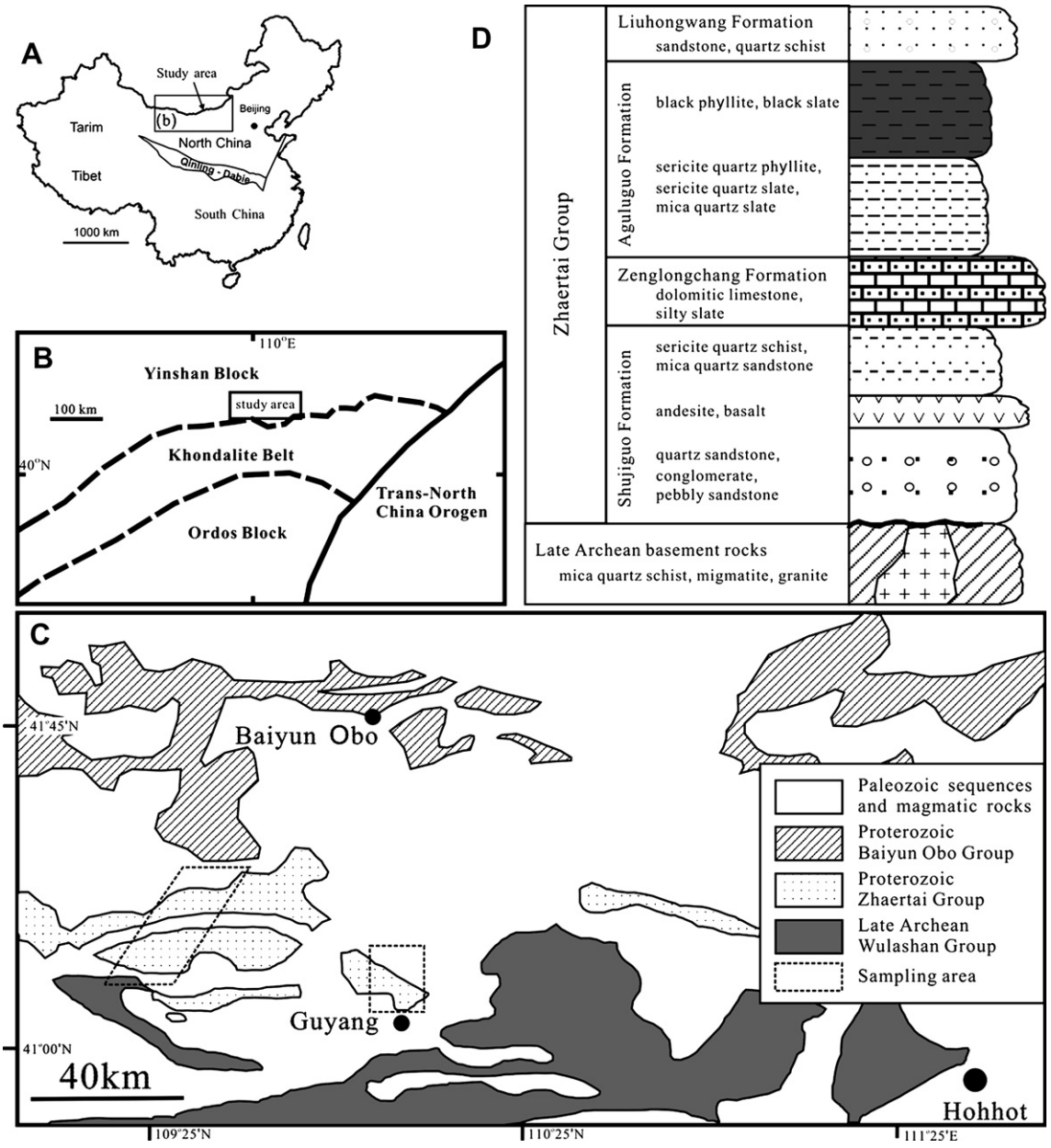

Fig. 1. (A) Sketch of major continental terrains in China. (B) Sketch of tectonic subdivision of the northwestern North China Craton (after Zhao et al., 2005). (C) Simplified geological map of the study area showing partly the Zhaertai and Baiyun Obo Groups (after Wang et al., 1992 and Zhang et al., 1999). (D) Simplified stratigraphic column showing major rock types of the Zhaertai Group and the underlying basement rocks (after Wang et al., 1992).

ranging from 1 to 3%. Trace (including rare earth) element concentrations were determined using an inductively coupled plasma mass spectrometer (ICP-MS). Samples were dissolved in a mixture of HF + HNO_3 within Teflon bombs for 5 days at a temperature of 200 °C. Analytical uncertainties for most elements are better than 5%.

3.2. Sm–Nd isotopic analysis

For Sm–Nd isotope analysis, rare earth elements were isolated on quartz columns by ion exchange chromatography with a 5-ml resin bed of AG 50 W-X12 (200–400 mesh). Nd and Sm were separated from other rare-earth elements on quartz columns using 1.7-ml Teflon powder coated with HDEHP, di(2-ethylhexyl)orthophosphoric acid, as cation exchange medium. Detailed chemical procedures are described in Chen et al. (2003). Measurements of Sm–Nd isotopic ratios were performed on a Finnigan MAT-262 mass spectrometer at the Laboratory for Radiogenic Isotope Geochemistry, IGG CAS. Sm and Nd were loaded as phosphate on pre-conditioned Re filaments and measured in a Re double filament configuration. $^{143}Nd/^{144}Nd$ ratios were normalized to $^{146}Nd/^{144}Nd = 0.7219$. Repeated measurements on the solution of the

Table 1
Localities and rock types of the analyzed samples

Sample No.	Rock type	Coordinates (Greenwich)	Formation
03ZT-24	Black slate	N41°06′19″; E110°03′09″	Agulugou
03ZT-23	Black slate	N41°05′56″; E110°03′15″	Agulugou
03ZT-22	Phyllite	N41°05′19″; E110°02′56″	Agulugou
03ZT-21	Pelitic sandstone	N41°05′19″; E110°02′56″	Agulugou
03ZT-20	Siltstone	N41°05′19″; E110°02′56″	Agulugou
03ZT-19	Quartz sandstone	N41°04′04″; E110°01′34″	Shujigou
03ZT-18	Pelitic sandstone	N41°03′57″; E110°01′31″	Shujigou
03ZT-17	Quartz sandstone	N41°03′57″; E110°01′31″	Shujigou
03ZT-16	Siltstone	N41°03′57″; E110°01′31″	Shujigou
03ZT-15	Quartz sandstone	N41°03′35″; E110°01′32″	Shujigou
04ZT-1	Basalt	N41°11′34″; E109°28′25″	Shujigou
03ZT-3	Basalt	N41°11′36″; E109°28′29″	Shujigou
03ZT-5	Basalt	N41°11′36″; E109°28′28″	Shujigou
03ZT-6	Basalt	N41°11′35″; E109°28′29″	Shujigou
03ZT-7	Basalt	N41°11′34″; E109°28′27″	Shujigou
03ZT-8	Basalt	N41°11′33″; E109°28′29″	Shujigou
03ZT-9	Basalt	N41°11′32″; E109°28′25″	Shujigou
03ZT-10	Quartz sandstone	N41°11′26″; E109°28′20″	Shujigou
03ZT-11	Quartz sandstone	N41°11′20″; E109°28′22″	Shujigou
03ZT-12	Migmatitic granite	N41°11′06″; E109°28′34″	Basement
03ZT-13	Migmatitic granite	N41°11′06″; E109°28′34″	Basement
03ZT-14	Migmatitic granite	N41°10′31″; E109°28′21″	Basement

Ames metal during 2004/2005 gave a mean value of 0.512149 ± 0.000022 ($n = 98$) for the $^{143}Nd/^{144}Nd$ ratio (Chen et al., 2007), close to the reference value of 0.512147 ± 0.000007 (Roddick et al., 1992). Results of repeated Sm–Nd analyses on the standard material BCR-1 (basalt powder) are also given in Chen et al. (2007). Total procedural blanks were <100 pg for Sm and Nd.

3.3. Zircon dating methods

Zircons were separated from the crushed rocks by conventional procedures. Zircon internal structures were studied using the cathodoluminescence technique (CL image) at the Institute of Geology and Geophysics, Chinese Academy of Sciences.

Zircon $^{207}Pb/^{206}Pb$ evaporation method: Detrital zircon grains from three quartzite samples were dated using the evaporation method following Kober (1986, 1987). Detailed analytical techniques are given in Chen et al. (2000, 2002). The GV IsoProbe-T mass spectrometer at the Laboratory for Radiogenic Isotope Geochemistry of the IGG CAS is equipped with a configuration of seven ion-counters. Intensities of Pb isotopes (^{204}Pb, ^{206}Pb, ^{207}Pb and ^{208}Pb) extruded from the evaporated zircon grain were statically measured using four ion-counters. Measurement of Pb isotopic ratios was simultaneously performed during heating of the zircon grain, without time-consuming evaporation-deposition cycles, as compared to conventional evaporation dating technique. Gain calibration of different ion-counters was done by measurements on Pb standard solutions (NBS981 and/or NBS982). Common Pb contribution was corrected using values of Stacey and Kramers (1975). Using this technique, variations of $^{207}Pb/^{206}Pb$ and $^{208}Pb/^{206}Pb$ ratios can be directly observed during the simultaneous evaporation and measurement run. These variations are related to the crystallization history and the U/Th ratio of zircon grains. More details on analytical techniques are given in Chen et al. (2005). During this study, standard zircon grains from Kuehl Lake/Canada (Zircon 91500) were measured and the results (mean $^{207}Pb/^{206}Pb$ age of 1062 ± 5Ma) are comparable to those reported by Wiedenbeck et al. (1995) and Chen et al. (2002). Ages obtained by the evaporation method are given as weighted average and errors refer to the 95% confidence level, calculated using the Isoplot program (Ludwig, 2001a).

Single-grain U–Pb dilution method: Detrital zircon grains from quartzite sample 03ZT-10 were dated by the single-grain U–Pb isotopic dilution method at the Institut für Geowissenschaften, Universität Tübingen, Germany. Isotope data were obtained using a Finnigan MAT-262 mass spectrometer. The analytical techniques are described in Chen et al. (2000, 2002). A factor of 1‰ per atomic mass unit for instrumental mass fractionation was applied to all Pb analysis, using NBS 981 as reference. Total procedural blanks are <10 pg for U and Pb. Initial common Pb remaining after correction for tracer and blank was corrected using values from the Stacey and Kramers (1975) model. Analytical data were evaluated using the Pbdat and ISOPLOT programs (Ludwig, 1988, 2001a). Errors are given as $2\sigma_m$.

Zircon SHRIMP U–Pb method: U–Th–Pb analyses of zircon grains from a migmatitic granite (sample 03ZT-14) were performed on a SHRIMP II in the Beijing SHRIMP Center. Relevant analytical procedures are described in Compston et al. (1984) and Williams (1998). Zircon grains were mounted in epoxy resin together with the Temora zircon standard and then polished down to half sections. The grains were documented by optical photomicrography and internal structures imaged by the CL. Measured isotope

ratios were corrected using a reference zircon (Temora, 417 Ma), whereas a zircon of known composition (SL13) was used to determine the U, Th and Pb content of the target. The data were corrected for common Pb, based on the measured ^{204}Pb, according to the Stacey and Kramers (1975) Pb evolution model. Isotopic ratios and single ages are quoted at the 1σ level. Data were calculated using the SQUID 1.0 (Ludwig, 2001b) and ISOPLOT (Ludwig, 2001a) software.

Zircon LA-ICP-MS U–Pb method: Zircon grains from basalt sample 04ZT01 were chosen for analysis using a laser ablation-inductively coupled plasma mass spectrometer (LA-ICP-MS) at the Northwest University, Xi'an, China. Zircon 91500 was employed as a standard and the standard silicate glass NIST was used to optimize the instrument. The analytical spot diameter was 30 μm. Raw data were processed using the GLITTER program and, as usually done for old rocks, the $^{207}Pb/^{206}Pb$ ratios were used to calculate corresponding age values. Detailed analytical techniques are described in Yuan et al. (2004).

3.4. Zircon Hf isotope analysis

Zircon Hf isotope analysis was carried out using a Geolas-193 laser-ablation microprobe, attached to a Neptune multi-collector ICP-MS at the IGG CAS. Instrumental conditions and data acquisition were described in Xu et al. (2004). The laser system delivers a beam of 193 nm UV light from an excimer laser. Each measurement was about 90 s with a 10 Hz repetition rate and a laser power of 100 mJ/pulse, resulting in 200 cycles of data. Sampling spots had beam diameters of 63 or 32 μm for small grains. Ar and He carrier gases were used to transport the ablated sample from the laser-ablation cell via a mixing chamber to the ICP-MS torch. Isobaric interference of ^{176}Lu on ^{176}Hf was corrected using the intensity of the interference-free ^{175}Lu isotope and a recommended $^{176}Lu/^{175}Lu$ ratio of 0.02655 (Machado and Simonetti, 2001), while isobaric interference of ^{176}Yb on ^{176}Hf isotope was corrected using the interference-free ^{172}Yb isotope and a recommended $^{176}Yb/^{172}Yb$ ratio of 0.5886 (Chu et al., 2002). Zircon 91500 was used as the reference standard during routine analyses, with a recommended $^{176}Hf/^{177}Hf$ ratio of 0.282293 ± 28 (Woodhead et al., 2004). Statistical data treatment was performed with the ISOPLOT program (Ludwig, 2001a,b). Data for chondrite from Blichert-Toft and Albarede (1998) were used to calculate the $\varepsilon_{Hf}(t)$ values. Single-stage model ages (T_{DM1}) were calculated following Griffin et al. (2000). Two-stage model ages (T_{DM2}) were calculated by assuming a mean $^{176}Lu/^{177}Hf$ value of 0.015 for average continental crust (Griffin et al., 2002).

4. Geochemical and Nd isotopic composition

Twenty-one representative samples were analyzed for major, trace, and rare earth element (REE) concentrations. Analytical data are given in Table 2. Whole-rock powders of twenty representative samples were measured for Nd isotopic composition and analytical results are given in Table 3.

4.1. Volcanic rocks

Six basalt samples were collected from intercalated volcanic layers in the lower part of the Shujigou Formation exposed about 40 km northwest of Guyang County. The analyzed samples contain 48.4–54.0 wt.% SiO_2, 2.8–3.3 wt.% MgO, 13.9–20.1 wt.% total FeO, and 4.7–5.1 wt.% K_2O+Na_2O. They are characterized by high TiO_2 and P_2O_5 contents of 2.2–2.8 wt.% and 1.2–1.5 wt.%, respectively. Total REE contents range from 422 to 477 ppm. Normalized trace element and REE compositions of six samples are plotted in Fig. 2A. All samples show strong fractionation between light and heavy REEs, having similar La_N/Yb_N ratios of 10.8–12.9 and slight Eu-depletion (Eu/Eu^* 0.88–0.95) probably indicating fractional crystallization of the parental basaltic magma. These samples exhibit depletion in Th, U, Nb, Ta, Zr, Hf, Ti and Sr when compared with the neighboring elements in the spidergram (Fig. 2B). Sm–Nd isotopic composition of six samples yielded ε_{Nd} values, calculated back to 1750 Ma of −8.49 to −7.97. When plotted in the initial ε_{Nd} value vs. SiO_2 diagram, no significant contamination of crustal material to the magma is indicated (Fig. 3).

4.2. Migmatitic granites

Three samples of migmatitic granites underlying the Zhaertai Group were collected from the same profile as the basalt samples. These samples contain 67.2–72.5 wt.% SiO_2, 14.0–16.0% wt.% Al_2O_3, and 6.9–9.2 wt.% K_2O+Na_2O and have A/CNK values of 1.01–1.22 and variable Na_2O/K_2O ratios. They have low total REE contents ranging from 57.8 to 87.1 ppm. The chondrite-normalized REE patterns demonstrate strong fractionation between the light and heavy REEs (Fig. 2C) with La_N/Yb_N values between 47.9 and 84.9 and strong Eu-enrichment (Eu/Eu^* 1.80–2.82). In the primitive mantle normalized geochemical spidergram (Fig. 2D), the migmatitic granite samples show pronounced negative Nb-, Ta-, and Ti-anomalies and slight positive Zr- and Hf-anomalies. Sm–Nd analysis of two migmatitic granite samples yields initial ε_{Nd} values of −1.44 and −0.08, when calculated back to 2500 Ma (formation age given below), probably implying significant contribution of mantle material to the magma of the granites.

4.3. Sedimentary rocks

Twelve samples of sedimentary rock collected from the Shujiguo and Aguluguo Formations were analyzed for geo-

Table 2
Major and trace element contents of whole-rock samples

Sample	Andesitic basalt						Migmatitic granite			Sandstone							Phyllite/slate				
	03ZT-3	03ZT-5	03ZT-6	03ZT-7	03ZT-8	03ZT-9	03ZT-12	03ZT-13	03ZT-14	03ZT-10	03ZT-11	03ZT-15	03ZT-16	03ZT-17	03ZT-18	03ZT-19	03ZT-20	03ZT-21	03ZT-22	03ZT-23	03ZT-24
SiO_2	50.37	49.58	49.84	48.43	51.36	54.04	67.21	72.45	72.19	71.32	85.93	76.27	73.32	90.52	71.71	91.07	55.58	82.95	68.19	75.65	78.86
TiO_2	2.68	2.63	2.76	3.33	2.76	2.24	0.34	0.14	0.22	0.18	0.08	0.09	0.21	0.06	0.32	0.06	0.90	0.42	0.76	0.55	0.50
Al_2O_3	12.11	12.06	11.68	11.02	11.76	12.08	15.96	14.06	13.95	15.83	6.63	12.36	14.14	4.45	15.31	1.21	21.99	8.36	17.37	11.69	9.83
Fe_2O_3	17.05	17.25	18.50	20.12	17.55	13.88	3.36	1.59	1.74	2.23	1.09	0.69	0.52	0.26	0.78	5.37	5.83	1.23	0.88	1.79	0.61
MnO	0.17	0.18	0.21	0.22	0.20	0.20	0.04	0.01	0.02	0.01	0.02	0.00	0.00	0.00	0.00	0.02	0.02	0.04	0.08	0.01	0.02
MgO	3.02	3.23	3.16	3.32	2.87	2.82	2.03	0.52	0.86	1.17	0.37	0.46	0.65	0.13	0.77	0.48	1.55	1.07	2.18	1.04	1.08
CaO	5.87	7.08	6.87	6.72	6.76	5.40	1.41	0.38	2.03	0.29	1.01	0.07	0.12	0.15	0.15	0.07	0.28	0.07	0.07	0.07	0.15
Na_2O	2.34	2.02	2.16	2.01	2.60	3.01	4.49	3.42	4.56	0.92	0.13	0.16	0.12	0.14	0.13	0.03	0.16	0.08	0.14	0.11	0.52
K_2O	3.04	2.65	2.33	2.09	1.94	2.70	2.88	5.76	2.36	5.06	2.23	8.58	9.05	3.26	9.31	0.43	8.28	3.07	6.41	3.63	2.58
P_2O_5	1.44	1.47	1.31	1.20	1.29	1.51	0.06	0.06	0.04	0.13	0.03	0.01	0.06	0.04	0.09	0.01	0.15	0.03	0.04	0.01	0.04
LOI	1.35	1.32	0.97	0.90	0.75	2.07	1.77	1.03	2.33	2.58	1.95	0.95	1.23	0.40	1.45	0.75	4.80	2.09	3.37	4.87	5.30
Total	99.44	99.46	99.79	99.36	99.83	99.95	99.53	99.42	100.3	99.72	99.46	99.64	99.43	99.41	100.0	99.50	99.53	99.40	99.49	99.42	99.48
A/CNK	0.68	0.63	0.63	0.62	0.63	0.68	1.22	1.12	1.01	2.11	1.49	1.28	1.38	1.10	1.45	1.88	2.26	2.33	2.38	2.76	2.51
Ba	1336	1368	1438	1345	986	1458	435	1263	796	1295	565	1139	1091	371	1110	74	515	389	570	455	378
Rb	72	67	58	50	43	47	81	101	45	118	73	146	136	43	152	27	132	108	246	156	130
Th	1.5	1.5	1.5	1.5	1.8	1.8	7.1	20.4	6.4	7.2	2.8	4.2	6.6	2.1	12.9	0.8	12.0	7.5	9.3	7.7	10.9
U	0.34	0.36	0.31	0.31	0.39	0.37	0.77	1.49	0.27	0.35	0.13	0.61	1.23	0.31	1.47	0.40	2.29	0.87	1.50	2.16	4.05
Nb	11.8	11.6	11.4	11.8	11.8	13.7	11.6	1.8	3.2	3.0	1.5	2.9	5.3	1.1	7.8	2.7	17.4	8.7	19.9	16.0	12.9
Ta	1.04	0.57	0.97	0.88	0.57	0.89	0.78	0.05	0.27	0.20	0.06	0.27	0.53	0.07	0.62	0.13	0.89	0.95	1.09	0.96	0.58
Pb	17.3	15.7	25.7	11.9	19.3	20.7	4.7	25.9	4.9	3.5	2.2	5.4	9.8	3.2	9.2	6.7	7.1	4.6	3.9	4.8	8.7
Sr	329	478	458	355	423	298	292	290	240	25	22	100	88	35	117	5.6	34	48	128	21	28
Zr	214	217	199	205	213	235	131	152	126	106	60	290	299	102	456	57	128	123	217	269	238
Hf	5.72	5.37	5.56	5.55	6.19	6.29	3.90	4.79	3.59	3.27	1.64	7.81	9.45	2.74	12.54	1.58	4.38	4.36	6.78	8.04	7.09
Y	42	42	41	40	41	45	3.4	2.9	3.2	6.3	3.4	5.9	6.7	5.4	8.0	5.5	16.5	8.7	12.7	8.9	20.6
Cs	2.67	2.60	2.22	1.88	1.42	1.41	4.77	0.21	0.17	0.67	0.18	0.85	1.39	1.13	1.62	3.01	4.85	4.52	9.26	4.49	5.10
La	59.15	68.28	64.78	61.41	69.17	73.34	20.8	25.2	16.7	32.0	6.9	14.5	19.1	8.7	29.3	1.5	42.6	21.1	21.1	2.2	10.7
Ce	130	146	138	126	142	150	40.1	39.1	26.9	50.8	10.8	27.1	39.2	18.4	57.8	3.3	82.0	39.5	43.8	4.4	25.9
Pr	17.01	18.31	17.49	16.32	18.88	18.76	4.36	4.42	2.63	6.54	1.34	3.14	4.76	2.00	7.34	0.38	11.43	4.37	5.15	0.57	3.15
Nd	68.7	76.3	72.0	69.7	75.2	75.2	11.21	13.7	8.2	21.1	4.7	11.8	17.3	7.4	29.0	1.4	42.3	14.8	19.4	2.4	13.1
Sm	12.75	13.54	12.94	12.42	13.52	14.04	1.28	1.57	0.97	3.00	0.79	1.99	2.80	1.03	4.70	0.31	7.60	2.45	3.18	0.65	3.15
Eu	3.30	3.78	3.57	3.45	3.75	3.69	0.72	0.78	0.72	0.99	0.27	0.67	0.82	0.28	1.06	0.10	1.68	0.47	0.59	0.19	0.62
Gd	10.41	10.97	10.41	9.93	11.02	10.97	1.12	1.01	0.62	2.18	0.56	1.28	1.63	0.66	2.15	0.44	5.34	1.89	2.31	0.83	3.26
Tb	1.42	1.45	1.34	1.30	1.52	1.42	0.13	0.11	0.07	0.27	0.06	0.17	0.21	0.08	0.26	0.07	0.74	0.27	0.37	0.18	0.57
Dy	7.57	8.00	7.62	7.41	8.43	8.17	0.50	0.52	0.32	1.37	0.33	0.84	1.25	0.41	1.45	0.45	4.34	1.60	2.37	1.42	3.69
Ho	1.52	1.57	1.48	1.45	1.78	1.59	0.10	0.09	0.06	0.25	0.07	0.16	0.26	0.09	0.28	0.09	0.89	0.32	0.51	0.35	0.78
Er	4.29	4.42	4.12	4.13	5.02	4.55	0.25	0.24	0.19	0.67	0.2	0.46	0.85	0.24	0.87	0.25	2.63	0.87	1.46	1.12	2.31
Tm	0.59	0.64	0.59	0.59	0.71	0.63	0.04	0.03	0.03	0.09	0.03	0.07	0.14	0.04	0.14	0.04	0.40	0.14	0.23	0.20	0.35
Yb	3.76	4.04	3.72	3.82	4.59	4.09	0.23	0.21	0.25	0.58	0.23	0.54	0.96	0.24	1.00	0.28	2.73	0.91	1.63	1.52	2.29
Lu	0.56	0.58	0.54	0.57	0.66	0.59	0.04	0.04	0.04	0.09	0.04	0.09	0.16	0.04	0.16	0.05	0.42	0.14	0.26	0.26	0.36
ΣREE	431.5	455.5	432.2	422.3	476.9	462.7	80.6	87.1	57.8	119.9	26.4	62.9	89.4	39.7	135.5	8.7	205.1	88.8	102.4	16.4	70.2
$(La/Yb)_n$	11.3	12.1	12.5	11.5	10.8	12.9	65.0	84.9	47.9	39.5	21.7	19.2	14.2	25.8	21.0	3.9	11.2	16.7	9.3	1.1	3.3
δEu	0.88	0.95	0.94	0.95	0.94	0.91	1.80	1.90	2.82	1.18	1.25	1.28	1.18	1.06	1.02	0.84	0.81	0.67	0.66	0.78	0.59

Major element contents in wt.% and trace element contents in ppm.
A/CNK: mole $Al_2O_3/(CaO+Na_2O+K_2O)$ ratio.

Table 3
Whole-rock Sm–Nd isotopic data

Sample	Rock type	Formation	Sm (ppm)	Nd (ppm)	$^{147}Sm/^{144}Nd$	$^{143}Nd/^{144}Nd$	T_{DM1} (Ga)	T_{DM2} (Ga)	$\varepsilon_{Nd\ (t)}$ 2500 Ma	$\varepsilon_{Nd(t)}$ 1750 Ma	$f_{Sm/Nd}$
03ZT-12	Granite	Basement	1.280	10.04	0.0771	0.510663 ± 10	2.76	2.86	−0.08	−11.73	−0.61
03ZT-13	Granite	Basement	1.750	15.02	0.0705	0.510484 ± 23	2.82	2.96	−1.44	−13.74	−0.64
03ZT-3	Basalt	Shujigou	13.40	73.52	0.1104	0.511227 ± 12	2.82	2.84		−8.17	−0.44
03ZT-5	Basalt	Shujigou	13.71	76.42	0.1086	0.511203 ± 13	2.81	2.84		−8.25	−0.45
03ZT-6	Basalt	Shujigou	12.92	72.14	0.1084	0.511215 ± 13	2.78	2.81		−7.97	−0.45
03ZT-7	Basalt	Shujigou	12.03	66.85	0.1090	0.511195 ± 9	2.83	2.86		−8.49	−0.45
03ZT-8	Basalt	Shujigou	12.95	72.30	0.1084	0.511192 ± 11	2.82	2.85		−8.42	−0.45
03ZT-9	Basalt	Shujigou	14.67	82.19	0.1080	0.511195 ± 12	2.80	2.83		−8.28	−0.45
03ZT-10	Sandstone	Shujigou	3.07	21.49	0.0863	0.510807 ± 10	2.79	2.88	−0.23	−10.98	−0.56
03ZT-11	Sandstone	Shujigou	0.82	5.10	0.0969	0.510898 ± 9	2.92	3.01	−1.87	−11.59	−0.51
03ZT-15	Sandstone	Shujigou	1.88	11.10	0.1028	0.511173 ± 8	2.70	2.73	1.64	−7.52	−0.48
03ZT-16	Sandstone	Shujigou	2.72	16.56	0.0993	0.511056 ± 12	2.77	2.83	0.47	−9.03	−0.50
03ZT-17	Sandstone	Shujigou	1.11	7.89	0.0855	0.510974 ± 46	2.57	2.60	3.31	−7.53	−0.57
03ZT-18	Sandstone	Shujigou	4.86	29.42	0.1000	0.511088 ± 17	2.75	2.79	0.87	−8.55	−0.49
03ZT-19	Sandstone	Shujigou	0.33	1.74	0.1147	0.511525 ± 61	2.49	2.49	4.67	−3.32	−0.42
03ZT-20	Siltstone	Agulugou	9.60	55.72	0.1043	0.511235 ± 12	2.65	2.67	2.37	−6.64	−0.47
03ZT-21	Pelitic	Agulugou	2.36	14.04	0.1017	0.511362 ± 11	2.42	2.41	5.70	−3.75	−0.48
03ZT-22	Phyllite	Agulugou	3.15	19.07	0.1001	0.511383 ± 10	2.36	2.33	6.64	−2.79	−0.49
03ZT-23	Shale	Agulugou	0.60	2.35	0.1551	0.511606 ± 42	3.98	3.40	−6.81	−10.85	−0.21
03ZT-24	Shale	Agulugou	3.06	11.84	0.1564	0.511606 ± 10	4.06	3.44	−7.21	−11.12	−0.21

chemical and Nd isotopic composition. The Shujiguo samples are mainly sandstones and the Aguluguo samples are sericite quartz phyllites and black graphite-bearing phyllites. Geochemical compositions of the analyzed samples are very variable with SiO_2-contents ranging from 55.6–1.1 wt.%, and total REE from 8.7 to 205 ppm. Most of the samples have slightly negative Eu-anomalies (Eu/Eu^* 0.59–1.25). Except for sample 03ZT-19 from the Shujiguo Formation and samples 03ZT-23 and 03ZT-24 from the Aguluguo Formation, other samples show strong fractionation between light and heavy REEs with La_N/Yb_N ratios ranging from 9.3 to 39.5. This holds particularly true for the Shujiguo sandstone samples (Fig. 4A and C). The REE contents and patterns of the phyllite samples (03ZT-20, 03ZT-21 and 03ZT-24) are similar to those of average continental crust (Taylor and McLennan, 1985). The Aguluguo phyllite samples have negative Nb-, Ta-, and Sr-anomalies (Fig. 4D), while the Shujiguo sandstone samples exhibit depletion in Nb, Ta, Ti, and Sr (Fig. 4B). Sm–Nd analyses of twelve samples yield variable initial Nd isotopic compositions (Fig. 3). Initial ε_{Nd} values range from −11.59 to −2.79, when calculated back to the mean deposition age of 1750 Ma.

5. Zircon ages

Detrital zircon grains from sandstone samples of the Shujiguo Formation were dated by the single grain U–Pb isotopic dilution method and the $^{207}Pb/^{206}Pb$ evaporation technique. Analytical data are given in Table 4 and 5, respectively. The SHRIMP U–Pb method and the LA-ICP-MS U–Pb method were used for zircons from the migmatitic granite sample and the basalt sample considering the possible complexity of the crystallization history of zircons from these samples. Dating results are given in Tables 6 and 7, respectively. Before dating, zircon grains were investigated for internal structure and crystallization history by means of the cathodoluminescence (CL) technique. CL images of zircon grains offer the opportunity to study their internal structure, which yields important information about the crystallization history of the grains (e.g., Hanchar and Miller, 1993; Pidgeon et al., 1998). CL images of the typical zircon populations are shown in Fig. 5.

5.1. Sedimentary rocks

Eleven detrital zircon grains from sandstone sample 03ZT-10 analyzed by ID-TIMS gave nearly concordant U–Pb ages (Table 4; Fig. 6) and $^{207}Pb/^{206}Pb$ ages cluster tightly around 2496 Ma to 2423 Ma. Similar ages were obtained from three other sandstone samples (03ZT-4, 03ZT-11 and 03ZT-15) by the single grain $^{207}Pb/^{206}Pb$ evaporation technique (Table 5). In total, forty seven grains gave $^{207}Pb/^{206}Pb$ ages ranging from 2527–2403 Ma, and most of them yield ages close to 2500 Ma (Fig. 7).

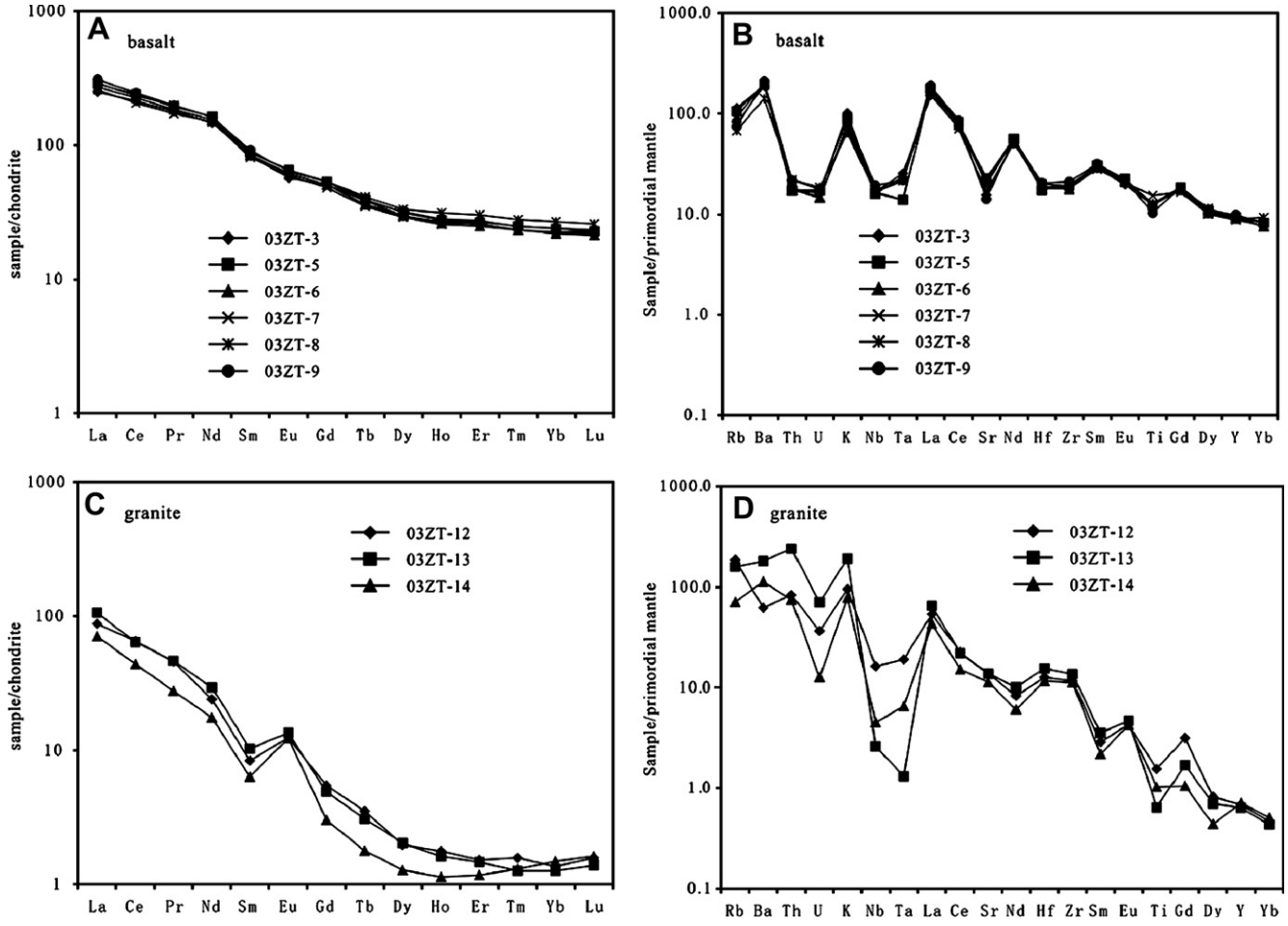

Fig. 2. Normalized rare earth and trace element contents of intercalated volcanic rocks of the Zhaertai Group and underlying migmatitic granites. Normalizing values for chondrite and primordial mantle are from Sun (1982) and Taylor and McLennan (1985).

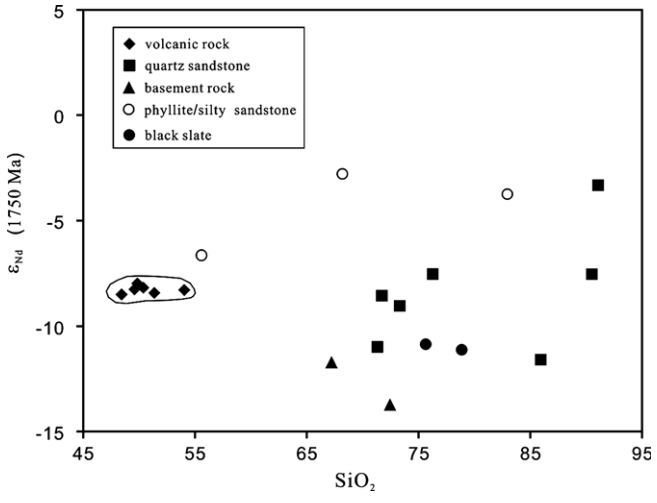

Fig. 3. Initial ε_{Nd} values vs. SiO_2 contents of the analyzed whole-rock samples. The initial ε_{Nd} values are calculated back to 1750 Ma.

5.2. Migmatitic granites

Zircon grains from sample 03ZT-14 are >150 μm in length and subhedral to euhedral in shape. The CL images show that most of the grains contain well-developed magmatic cores with oscillatory zoning surrounded by a recrystallized rim (Fig. 5). Twelve analytical spots gave nearly concordant U–Pb SHRIMP ages ranging from 2450 to 2580 Ma (Table 6; Fig. 8), with a mean $^{207}Pb/^{206}Pb$ age of 2511 ± 26 Ma. When plotted in the concordia diagram, the data fall in two groups (Fig. 8), although no significant difference can be observed in U, Th contents and Th/U ratios. These two groups give mean $^{207}Pb/^{206}Pb$ ages of 2480 ± 13 Ma and 2564 ± 19 Ma. Considering that the granite body underwent strong migmatization, the older age can be interpreted as the formation age of the granite and the age of 2480 Ma may represent the time of migmatization.

5.3. Volcanic rocks

Basalt sample 04ZT-1 contains a small amount of tiny zircon grains that probably have a complicate history as indicated from the internal structures shown in CL images. Seventeen grains were analyzed by the LA-ICP-MS U–Pb method and, as shown in Fig. 9, most analytical spots gave concordant U–Pb ages. Sixteen out of

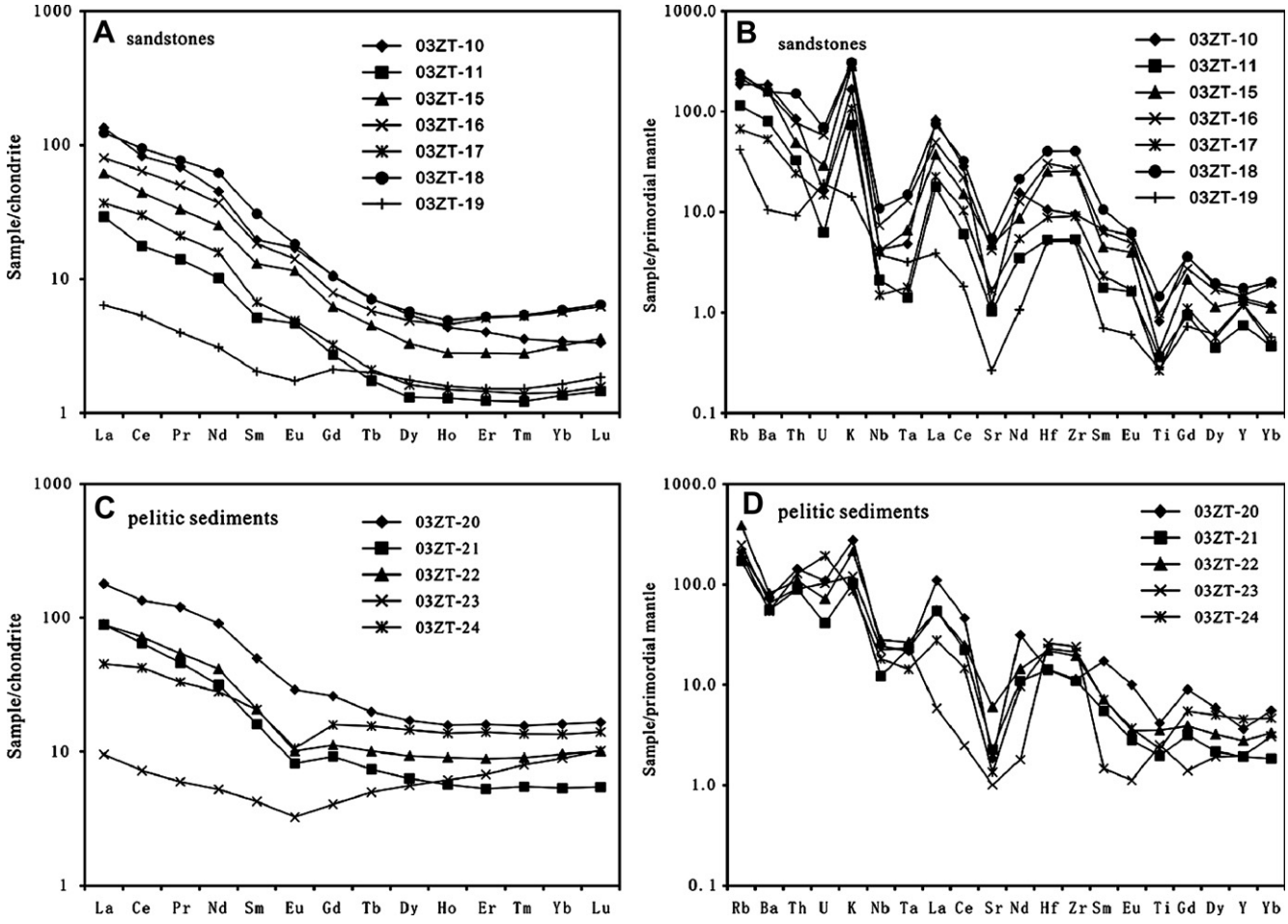

Fig. 4. Normalized rare earth and trace element contents of sandstone and pelitic rock samples of the Zhaertai Group. Normalizing values for chondrite and primordial mantle are from Sun (1982) and Taylor and McLennan (1985).

Table 4
Zircon U–Pb dilution data of quartzite sample 03ZT-10 of the Zhaertai Group

No.	Measured	U	Pb	Atomic ratios				Apparent ages (Ma)		
				$^{208}Pb^*/^{206}Pb^*$	$^{206}Pb^*/^{238}U$	$^{207}Pb^*/^{235}U$	$^{207}Pb^*/^{206}Pb^*$	$^{206}Pb^*/^{238}U$	$^{207}Pb^*/^{235}U$	$^{207}Pb^*/^{206}Pb^*$
1	2117	222	112	0.13	0.4429	9.706	0.15892	2363	2407	2444
2	4071	296	164	0.27	0.4450	9.631	0.15701	2373	2400	2423
3	6758	220	122	0.14	0.4934	10.956	0.16103	2586	2519	2467
4	11468	467	249	0.15	0.4685	10.495	0.16254	2477	2480	2482
5	11986	144	81	0.24	0.4642	10.330	0.16144	2458	2465	2470
6	4587	95	56	0.21	0.5002	11.155	0.16172	2615	2536	2474
7	8173	146	72	0.16	0.4311	9.7191	0.16353	2311	2409	2492
8	5286	207	111	0.21	0.4486	9.9710	0.16124	2389	2432	2468
9	2840	187	83	0.15	0.3887	8.5635	0.15986	2117	2293	2453
10	8067	311	142	0.11	0.4159	9.0610	0.15801	2242	2344	2434
11	26545	245	126	0.13	0.4599	10.389	0.16382	2439	2470	2496

seventeen analytical spots have $^{206}Pb/^{238}Pb$ ages between 2536 Ma and 2134 Ma, only one spot yielded young, concordant U–Pb ages of 1743 Ma. Taking into consideration that the sedimentary rocks of the Zhaertai Group and the underlying migmatitic granites contain abundant zircon grains of late Archean to early Paleoproterozoic age, it is reasonable to suggest that the 2536 Ma and 2134 Ma zircon grains originated from basement rocks during ascent of the basaltic magma. The volcanism likely took place around 1750 Ma, being contemporaneous with the mafic dyke swarm within the North China Craton (e.g., Peng et al., 2005; Wang et al., 2004).

Table 5
Zircon evaporation data of three quartzite samples from the Zhaertai Group

Grain No.	No. of ratios	Mean value of $^{207}Pb/^{206}Pb$ ratios	$^{207}Pb/^{206}Pb$ age (Ma)	Th/U
03ZT-4				
1	152	0.16236 ± 5	2480 ± 1	0.20
2	152	0.16284 ± 7	2485 ± 1	0.23
3	76	0.15661 ± 19	2419 ± 2	0.49
4	166	0.15592 ± 28	2412 ± 3	0.57
5	76	0.16426 ± 5	2500 ± 1	0.25
6	114	0.15659 ± 15	2419 ± 2	0.65
7	152	0.15603 ± 16	2413 ± 2	2.17
8	114	0.16409 ± 22	2498 ± 2	0.38
9	114	0.15888 ± 25	2444 ± 3	0.46
10	190	0.15648 ± 15	2418 ± 2	0.40
11	76	0.16297 ± 30	2487 ± 3	0.36
12	182	0.16298 ± 16	2487 ± 2	0.27
13	152	0.16086 ± 46	2465 ± 5	0.47
14	190	0.16378 ± 10	2495 ± 1	0.46
15	114	0.15729 ± 21	2427 ± 2	0.23
16	188	0.16040 ± 20	2460 ± 2	0.50
03ZT-11				
1	190	0.15820 ± 15	2427 ± 2	0.43
2	110	0.15514 ± 5	2403 ± 1	0.38
3	152	0.16426 ± 7	2500 ± 1	0.28
4	112	0.16399 ± 5	2497 ± 1	0.24
5	152	0.16110 ± 18	2467 ± 2	0.38
6	112	0.16028 ± 8	2459 ± 1	0.64
7	150	0.15897 ± 7	2445 ± 1	0.49
8	150	0.15766 ± 5	2431 ± 1	0.17
9	114	0.16362 ± 10	2493 ± 1	0.29
10	150	0.16225 ± 16	2479 ± 2	0.61
11	190	0.16305 ± 19	2488 ± 2	0.34
12	74	0.16316 ± 37	2489 ± 4	0.78
13	224	0.16449 ± 5	2502 ± 1	0.58
14	112	0.16218 ± 23	2479 ± 2	0.45
15	38	0.16479 ± 61	2505 ± 6	0.46
16	114	0.16328 ± 10	2490 ± 1	0.60
17	114	0.16342 ± 29	2491 ± 3	0.51
18	114	0.16213 ± 13	2478 ± 1	0.39
19	114	0.16531 ± 20	2511 ± 2	0.62
03ZT-15				
1	152	0.16397 ± 23	2497 ± 2	0.64
2	114	0.16620 ± 45	2524 ± 5	0.74
3	114	0.16673 ± 37	2525 ± 4	0.61
4	114	0.16445 ± 16	2502 ± 2	0.87
5	190	0.16562 ± 6	2510 ± 1	0.80
6	110	0.16447 ± 30	2502 ± 3	0.46
7	150	0.16216 ± 7	2489 ± 1	0.20
8	38	0.16460 ± 120	2504 ± 12	0.71
9	228	0.16554 ± 10	2513 ± 1	0.62
10	104	0.16540 ± 54	2512 ± 6	0.69
11	102	0.16479 ± 56	2505 ± 6	0.48
12	148	0.16694 ± 32	2527 ± 3	0.70

A similar U–Pb age of 1728 ± 5 Ma has been reported for basalts of the low part of the Baiyun Obo Group and was interpreted as a product of rifting along the cratonic margin (Lu et al., 2002).

6. Zircon Hf isotopic data

The Lu–Hf isotopic system of zircon is well known to have a high isotopic closure temperature. Therefore, zircon Hf isotopic compositions can preserve source information, even for high-grade metamorphic rocks (e.g., Scherer et al., 2000). Owing to the high mechanical and chemical resistance of zircons during erosion, transportation and sedimentation, Hf isotopic composition of detrital zircon grains can be an ideal indicator for source characteristics of sedimentary rocks. In this study, eighty five detrital zircon grains from four sandstone samples (03ZT-4, 03ZT-10, 03ZT-11 and 03ZT15) were analyzed using the LA-ICP-MS method and analytical data are given in Table 8. Except for two zircon grains having highly negative initial ε_{Hf} values (−13.4 and −14.6), the analyzed grains gave initial ε_{Hf} values ranging about from −4 to +7, with a peak value of about +4 (Fig. 10A), when calculated back to 2500 Ma. These two grains with highly negative initial ε_{Hf} values give $T_{DM2}(Hf)$ values of about 3800 Ma, indicating an approximation for the source age of the host magma from which the negative ε_{Hf} (t) zircon grains crystallized (Zheng et al., 2006). Other zircon grains give $T_{DM1}(Hf)$ values between about 2900 Ma to 2500 Ma, clustering around 2700 Ma (Fig. 10B), similar to the $T_{DM}(Nd)$ values of the whole-rock samples. A close match between the U–Pb ages and $T_{DM1}(Hf)$ ages with positive initial ε_{Hf} values for about ninety percent of the zircon grains suggests growth and/or prompt reworking of a juvenile crustal section and further indicates a major mantle contribution to magmas of the protoliths of sedimentary rocks, which provided the detrital zircon grains (Zheng et al., 2006; Wu et al., 2006).

7. Discussion

7.1. Timing of mesoproterozoic rifting and sedimentation

The Zhaertai Group is commonly interpreted as a Mesoproterozoic sedimentary sequence deposited in the so-called Zhaertai basin, being a branch of the Mesoproterozoic Langshan-Baiyun Obo rift system (Wang et al., 1992). Isotopic dating results of this group, reported mainly in internal reports of the Geological Survey of Inner Mongolia from 1970 to 1980, gave controversial age constraints on the deposition time, ranging from Paleoproterozoic to early Paleozoic (data compiled in Wang et al., 1992). These age data were mainly obtained by K–Ar on whole-rock and mica, Pb–Pb on whole-rock, galena, and pyrite minerals from different parts of the Zhaertai Group. The K–Ar and U–Pb isotopic systems can be strongly influenced by later overprints, as isotopic closure temperatures of these systems are commonly low (Mezger, 1990 and references therein). As mentioned above, intercalated andesitic to basaltic volcanic rocks were found in the

Table 6
Zircon SHRIMP U- Pb data of migmatitic granite sample 03ZT-14

Spot No.	$^{206}Pb_c$ (%)	U (ppm)	Th (ppm)	Th/U	$^{206}Pb^a$ (ppm)	$^{207}Pb^a/^{206}Pb^a$ (error %)	$^{206}Pb^a/^{238}U$ (error %)	$^{207}Pb^a/^{235}U$ (error %)	$^{207}Pb^a/^{206}Pb^a$ (Ma)
1	0.23	202	181	0.92	77.9	0.1664 (0.6)	0.447 (2.9)	10.25 (3.0)	2522 ± 11
2	0.20	267	263	1.02	111	0.1692 (0.6)	0.481 (2.9)	11.23 (3.0)	2550 ± 10
3	0.19	327	314	0.99	143	0.1653 (0.5)	0.507 (2.9)	11.56 (2.9)	2511 ± 7.6
4	0.19	347	267	0.79	141	0.1601 (0.5)	0.473 (2.9)	10.43 (2.9)	2456 ± 8.8
5	0.09	460	137	0.31	174	0.1639 (0.4)	0.440 (2.9)	9.94 (2.9)	2496 ± 6.7
6	0.11	292	271	0.96	130	0.1707 (0.4)	0.516 (2.9)	12.14 (2.9)	2565 ± 7.5
7	0.26	121	92	0.78	51.1	0.1690 (0.7)	0.490 (2.9)	11.42 (3.0)	2548 ± 13
8	0.08	732	150	0.21	289	0.1615 (0.3)	0.459 (2.9)	10.22 (2.9)	2471 ± 5.2
9	0.13	499	515	1.07	197	0.1630 (0.4)	0.458 (2.9)	10.30 (2.9)	2487 ± 6.2
10	0.12	296	180	0.63	117	0.1614 (0.6)	0.460 (2.9)	10.24 (3.0)	2470 ± 11
11	0.17	827	634	0.79	305	0.1627 (0.3)	0.429 (2.9)	9.62 (2.9)	2483 ± 4.8
12	0.12	327	454	1.43	140	0.1717 (0.4)	0.498 (2.9)	11.79 (2.9)	2574 ± 7.2

Errors are given at 1σ level; Pb_c = common Pb.
[a] Pb = radiogenic Pb; Standard error is 0.26%.

Table 7
Zircon U–Pb LA-ICP-MS data of basalt sample 04ZT-01

Grain No.	Ratios				Ages (Ma)		
	Th/U	$^{206}Pb/^{238}U$	$^{207}Pb/^{235}U$	$^{207}Pb/^{206}Pb$	$^{206}Pb/^{238}U$	$^{207}Pb/^{235}U$	$^{207}Pb/^{206}Pb$
1	0.20	0.4541 (40)	9.781 (85)	0.1561 (15)	2414 (18)	2414 (8)	2414 (7)
2	0.24	0.4688 (41)	10.51 (9)	0.1624 (16)	2478 (18)	2480 (8)	2481 (7)
3	0.83	0.4713 (42)	10.60 (9)	0.1631 (16)	2489 (18)	2489 (8)	2488 (7)
4	0.49	0.4499 (40)	9.585 (83)	0.1544 (15)	2395 (18)	2396 (8)	2396 (7)
5	0.25	0.4494 (40)	9.549 (82)	0.1540 (15)	2393 (18)	2392 (8)	2391 (7)
6	0.35	0.4443 (39)	9.328 (81)	0.1522 (15)	2370 (17)	2371 (8)	2371 (7)
7	0.51	0.4776 (41)	10.93 (10)	0.1660 (16)	2517 (18)	2518 (8)	2518 (7)
8	0.65	0.4820 (42)	11.16 (10)	0.1679 (16)	2536 (18)	2537 (8)	2537 (7)
9	0.57	0.4670 (43)	10.52 (9)	0.1634 (16)	2470 (18)	2482 (8)	2491 (7)
10	0.17	0.4591 (40)	10.00 (9)	0.1580 (16)	2435 (18)	2435 (7)	2434 (6)
11	0.53	0.4328 (36)	8.778 (68)	0.1477 (14)	2318 (16)	2315 (7)	2319 (6)
12	0.61	0.4633 (39)	10.20 (8)	0.1602 (15)	2454 (17)	2453 (7)	2457 (6)
13	0.86	0.4230 (36)	9.657 (76)	0.1632 (15)	2306 (16)	2403 (7)	2489 (7)
14	0.24	0.3105 (26)	4.564 (36)	0.1067 (10)	1743 (13)	1743 (7)	1743 (7)
15	0.43	0.4825 (42)	11.20 (9)	0.1681 (15)	2538 (18)	2540 (8)	2539 (7)
16	0.40	0.3925 (35)	8.483 (89)	0.1567 (21)	2134 (16)	2284 (10)	2421 (24)
17	1.25	0.4654 (41)	10.37 (8)	0.1611 (14)	2464 (18)	2469 (8)	2467 (7)

lower part of this group and dating of such volcanic rocks can provide age constraints on the lower limit of deposition. However, the analyzed basalt sample contains abundant old zircon grains (late Archean to early Paleoproterozoic in age) possibly originating from the basement rocks underlying the study area. Only one zircon grain yields a U–Pb age of 1743 Ma that is tentatively interpreted as formation age of the basaltic layer. Arguments in favor for this interpretation are that metamorphism of the Zhaertai Group was not high enough to reset the zircon U–Pb isotopic system and that mafic dikes of pre-Mesoproterozoic age found in the North China Craton commonly underwent high-grade metamorphism up to granulite-facies (e.g., Peng et al., 2005; Guo et al., 2002). If we accept the age of the basalt, then deposition of the Zhaertai Group and opening of the Langshan-Baiyun Obo ocean (or rift system) should have started shortly before 1743 Ma.

Basalt samples analyzed in this study are characterized by high contents of FeO_T, TiO_2 and P_2O_5 and low initial ε_{Nd} values. All samples have high REE-contents, negative Nb and Ta anomalies and exhibit strong fractionation between light and heavy REEs (La_N/Yb_N ratios 10.8–12.9), likely indicating fractional differentiation of the parental magma source. Similar features can be found in evolved mafic dykes from other localities within the North China Craton. Those dykes are commonly unmetamorphosed and were dated between about 1780 and 1750 Ma by the Ar–Ar and SHRIMP methods (Peng et al., 2005; Peng, 2005; Wang et al., 2004). These magmatic rocks are interpreted as products related to the breakup of the Paleoproterozoic supercontinent Columbia (e.g., Peng

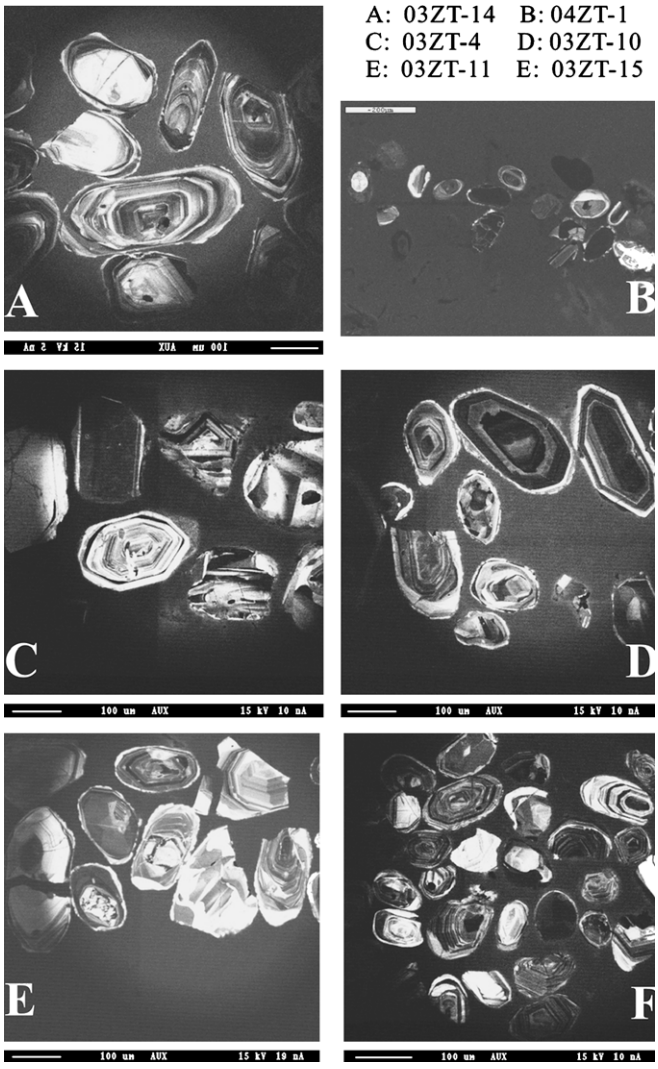

Fig. 5. Cathodoluminescence images of typical populations of zircon grains of migmatitic granite sample 03ZT-14 and basalt sample 04ZT-1 and detrital zircon grains of sandstone samples 03ZT-4, 03ZT-10, 03ZT-11, and 03ZT-15.

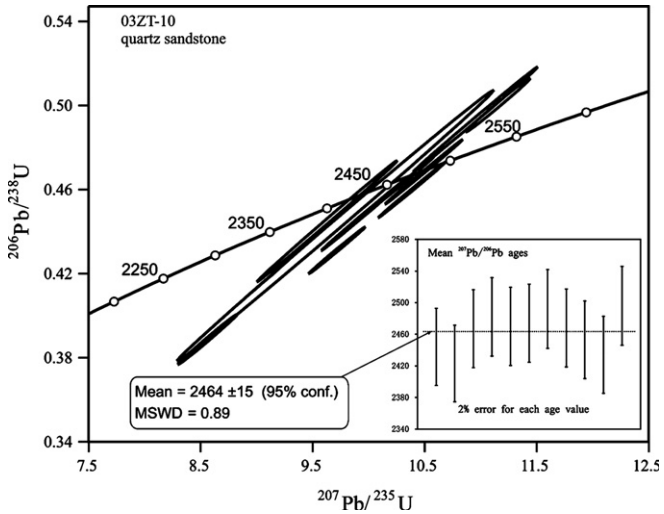

Fig. 6. Zircon U–Pb concordia diagram for sandstone sample 03ZT-10. Data were obtained using the U–Pb isotopic dilution method and give a mean $^{207}Pb/^{206}Pb$ age value of 2464 ± 15 Ma (MSWD = 0.89).

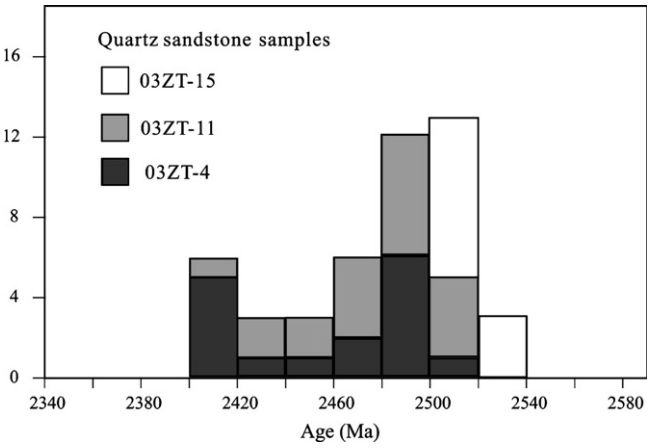

Fig. 7. Frequency histogram of zircon $^{207}Pb/^{206}Pb$ ages of sandstone samples 03ZT-4, 03ZT-11, and 03ZT-15, obtained by the evaporation method. Age values cluster around 2500 Ma.

et al., 2005) or to post-collision extensional collapse after amalgamation of the Eastern and Western Blocks along the Central Zone of the North China Craton during the late Paleoproterozoic (Wang et al., 2004; Zhao et al., 1998, 1999, 2000, 2001, 2002, 2005). Negative initial ε_{Nd} values of the basalt samples (−8.49 to −7.97 at 1750 Ma) suggest an origin from an enriched mantle source; crustal contamination is less important, as shown in the initial ε_{Nd} value vs. SiO_2 diagram (Fig. 3). The enriched mantle could have resulted from subduction of old crustal material before amalgamation of the Eastern and Western Blocks or from delamination of the lower crustal section before breakup of the supercontinent. Such low initial ε_{Nd} (1750 Ma) values of the basalts require a highly enriched mantle (or mantle domain) as a magma source. Previous studies showed that the old middle/lower crust of the North China Craton is characterized by low ε_{Nd} values

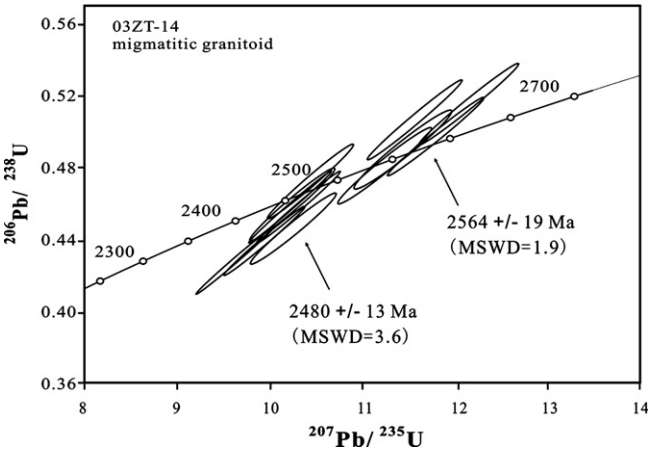

Fig. 8. Zircon U–Pb concordia diagram for migmatitic granite sample 03ZT-14. Data were obtained using the SHRIMP U–Pb method and cluster in two groups, giving mean $^{207}Pb/^{206}Pb$ age values of 2480 ± 13 Ma (MSWD = 3.6) and 2564 ± 19 Ma (MSWD = 1.9), respectively.

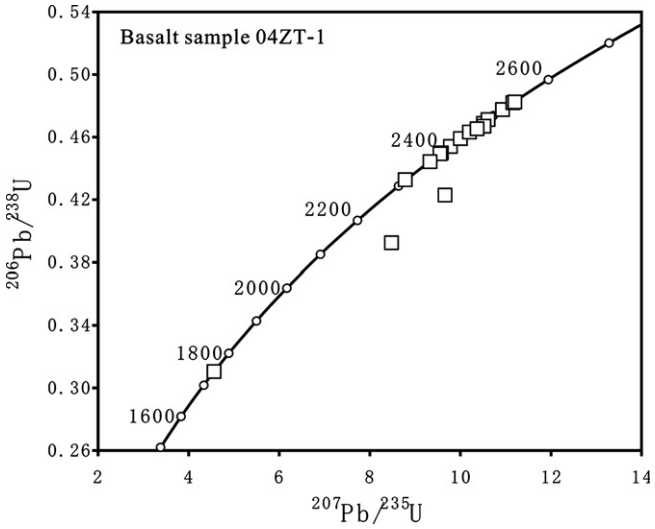

Fig. 9. Zircon U–Pb concordia diagram for basalt sample 04ZT-1. Data were obtained using the LA-ICP-MS U–Pb method. One zircon grain gave concordant U–Pb ages of 1743 Ma, the other grains yielded $^{207}Pb/^{206}Pb$ age values between 2300 and 2600 Ma.

(around −40) at present (Jahn and Zhang, 1984). This strong mantle enrichment in the Mesoproterozoic can be realized if a huge volume of pre-Mesoproterozoic crustal material was subducted or an old lower crustal section of the North China Craton was delaminated.

7.2. Sedimentary source

Owing to their highly physical and chemical resistance and high closure temperature of the U–Pb and Lu–Hf isotopic systems, zircons have become a powerful tool for provenance studies of geologic terrains, and for constraining the depositional ages and sources of sediments (e.g., Nelson, 2001; Valverde et al., 2000). Principles of the application are based on two major facts (1) that zircon grains can preserve age information during erosion, transportation, diagenesis, and even metamorphic overprint of the sediments and, (2) that different geological terranes exhibit distinguishable evolution histories (e.g., Valverde et al., 2000). The zircon Lu–Hf isotopic system has a very high isotopic closure temperature such that the Hf isotopic composition of zircon can preserve source information, even for high-grade metamorphic rock, such as granulites (Scherer et al., 2000). Therefore, Hf isotopic compositions of detrital zircon grains, combined with whole-rock Sm–Nd data, are useful for revealing source characteristics of sedimentary rocks. Nd isotopic compositions of sedimentary rocks can provide useful information about the formation and evolution of the continental crust, owing to the relatively immobile behavior of the Sm–Nd isotopic system (e.g., Liew and Hofmann, 1988; DePaolo et al., 1991). Initial $^{143}Nd/^{144}Nd$ isotopic ratios (ε_{Nd}) and depleted-mantle model ages (T_{DM}) characterize sedimentary source rock features and therefore have been widely applied to studies on the tectonic evolution of continental blocks.

The North China Craton is characterized by Archean to Paleoproterozoic basement rocks, which mainly underwent four major tectonothermal events during 3.0–2.9 Ga, 2.6–2.5 Ga, 2.4–2.3 Ga, and 1.8 –1.7 Ga (e.g., Ma and Bai, 1998; Ma et al., 1987; Yang et al., 1986). Detrital zircons from sedimentary rocks (mainly sandstone) of the lower part of the Zhaertai Group yield consistent ages of about 2500 Ma obtained by using the evaporation and ID-TIMS method (Figs. 6 and 7), implying a homogeneous source terrane at the beginning of rifting. Sedimentation analysis suggests northward transport of material (Wang et al., 1992), therefore, it is reasonable to trace the source material southwards in the North China Craton, where late Archean basement rocks are widely distributed (e.g., Kröner et al., 1988, 2005; Wilde et al., 2002, 2005). At the northwestern margin of the North China Craton, termed the Yinshan terrane by Zhao et al. (2005), late Archean magmatic rocks are also found. For instance, the Guyang-Wuchuan complex and the Sheerteng complex are located south of the study area. Detrital zircon grains from sandstones of the Zhaertai Group have high initial ε_{Hf} values (mostly >0, calculated back to 2500 Ma) and most of the sandstone samples also have positive initial ε_{Nd} (2500 Ma) values, implying a mantle origin for the protoliths. The basement rocks (migmatitic granites) directly underlying the Zhaertai Group also yield ages of about 2500 Ma using the SHRIMP U–Pb method (Fig. 8). These rocks probably underwent migmatitization shortly after 2500 Ma. This observation points to an important crustal growth and thermal event that took place in the late Archean along the northwestern margin of the North China Craton or the Yinshan terrane. Recent geochronological studies have shown that high-grade metasedimentary rocks in the Khondalite Belt (Zhao et al., 2005), south to the Yinshan terrane, contain abundant Paleoproterozoic zircon grains (Xia et al., 2006a,b). However, Paleoproterozoic detrial zircons have not been detected in sandstones of the Zhaertai Group. This could imply (1) that Paleoproterozoic magmatism was much weaker at the northern margin of the North China Craton than in its inner parts or (2) that Paleoproterozoic basement rocks were not exposed at the surface at least during the beginning of the rifting. The first possibility implies that the evolution of the Yinshan terrane in the tectonic subdivision of Zhao et al. (2005) was different from that of the other parts of the North China Craton.

The initial ε_{Nd} values (1750 Ma) of the eighteen sedimentary rock and basalt samples collected from the Zhaertai Group increase upwards through the stratigraphic sequence (Fig. 11). The sandstone samples (03ZT-10 and 03ZT-11) from the lower section yield initial ε_{Nd} values close to those of the underlying migmatitic granites, a representative basement source of the sedimentary material. Sandstones of the upper Shujigou

Table 8
Zircon Lu–Hf isotopic data of four quartzite samples

Spot No.	$^{176}Yb/^{177}Hf$	$^{176}Lu/^{177}Hf$	$^{176}Hf/^{177}Hf$	Error ($2\sigma_m$)	$\varepsilon_{Hf}(0)$	$\varepsilon_{Hf}(t)$ (2.5Ga)	T_{DM1} (Ma)	T_{DM2} (Ma)
03ZT-4								
1	0.023620	0.000663	0.281307	0.000028	−51.8	2.2	2692	2835
2	0.012044	0.00037 7	0.281285	0.000032	−52.6	1.9	2701	2852
3	0.013253	0.000388	0.281264	0.000031	−53.3	1.2	2731	2900
4	0.031276	0.000885	0.281374	0.000035	−49.5	4.2	2617	2712
5	0.012850	0.000375	0.281200	0.000026	−55.6	−1.1	2816	3038
6	0.013032	0.000392	0.281315	0.000021	−51.5	3.0	2662	2788
7	0.013214	0.000403	0.281269	0.000029	−53.2	1.3	2725	2891
8	0.016860	0.000504	0.281357	0.000024	−50.1	4.3	2614	2710
9	0.037368	0.000932	0.281419	0.000032	−47.8	5.8	2558	2616
10	0.018979	0.000551	0.281288	0.000025	−52.5	1.7	2710	2864
11	0.030834	0.000853	0.281313	0.000021	−51.6	2.1	2697	2840
12	0.019865	0.000575	0.281312	0.000028	−51.6	2.6	2679	2813
13	0.023541	0.000717	0.281290	0.000029	−52.4	1.5	2718	2876
14	0.039541	0.001138	0.281388	0.000026	−49.0	4.3	2615	2707
15	0.048191	0.001454	0.281438	0.000032	−47.2	5.6	2567	2628
16	0.012425	0.000362	0.281345	0.000022	−50.4	4.1	2620	2720
17	0.020178	0.000611	0.281301	0.000021	−52.0	2.1	2696	2842
18	0.012661	0.000364	0.281321	0.000021	−51.3	3.2	2653	2774
19	0.031687	0.000894	0.281367	0.000019	−49.7	4.0	2626	2726
20	0.080582	0.002389	0.281484	0.000029	−45.5	5.6	2567	2624
21	0.028908	0.000779	0.281263	0.000023	−53.4	0.5	2760	2942
22	0.012524	0.000444	0.281323	0.000024	−51.2	3.2	2655	2777
03ZT-10								
1	0.009906	0.000319	0.281257	0.000023	−53.6	1.2	2736	2902
2	0.017126	0.000478	0.281312	0.000027	−51.6	2.9	2673	2798
3	0.052754	0.001709	0.281399	0.000030	−48.6	4.0	2639	2735
4	0.031229	0.000818	0.281309	0.000040	−51.7	2.3	2700	2840
5	0.014795	0.000489	0.281301	0.000034	−52.0	2.5	2688	2823
6	0.010831	0.000369	0.281272	0.000037	−53.0	1.7	2718	2873
7	0.018119	0.000555	0.281285	0.000044	−52.6	1.9	2714	2864
8	0.045001	0.001078	0.281349	0.000076	−50.3	3.2	2664	2779
9	0.031457	0.000861	0.281293	0.000054	−52.3	1.6	2725	2879
10	0.021850	0.000684	0.281295	0.000053	−52.2	2.0	2710	2856
11	0.015313	0.000517	0.281307	0.000034	−51.8	2.7	2682	2813
12	0.014545	0.000450	0.281262	0.000032	−53.4	1.2	2738	2904
13	0.027424	0.000752	0.281342	0.000029	−50.6	3.6	2650	2760
14	0.064461	0.001660	0.281446	0.000031	−46.9	5.7	2571	2628
15	0.010860	0.000312	0.281283	0.000025	−52.7	2.2	2700	2845
16	0.005299	0.000182	0.281295	0.000026	−52.2	2.8	2675	2804
17	0.043926	0.001218	0.281312	0.000027	−51.6	1.7	2724	2874
18	0.020150	0.000626	0.281170	0.000022	−56.7	−2.4	2875	3123
19	0.024511	0.000711	0.281310	0.000024	−51.7	2.5	2691	2826
20	0.012949	0.000401	0.281298	0.000022	−52.1	2.6	2686	2821
21	0.018345	0.000540	0.281304	0.000028	−51.9	2.5	2688	2822
03ZT-11								
1	0.023883	0.000990	0.281210	0.000101	−55.3	−1.6	2848	3074
2	0.017840	0.000599	0.281260	0.000169	−53.5	0.9	2752	2925
3	0.016714	0.000539	0.281255	0.000023	−53.6	0.8	2753	2929
4	0.020994	0.000656	0.281343	0.000025	−50.5	3.7	2643	2748
5	0.044059	0.001189	0.281375	0.000032	−49.4	4.0	2635	2733
6	0.036841	0.001017	0.280879	0.000028	−66.9	−13.4	3297	3791
7	0.012449	0.000402	0.281294	0.000022	−52.3	2.4	2691	2829
8	0.011347	0.000330	0.281262	0.000024	−53.4	1.4	2729	2892
9	0.020169	0.000718	0.280831	0.000299	−68.7	−14.6	3337	3866
10	0.024108	0.000704	0.281338	0.000052	−50.7	3.5	2653	2765
11	0.010094	0.000396	0.281272	0.000059	−53.0	1.7	2721	2877
12	0.012720	0.000492	0.281118	0.000089	−58.5	−4.0	2934	3221
13	0.005765	0.000261	0.281168	0.000116	−56.7	−1.8	2849	3088
14	0.047146	0.001604	0.281272	0.000162	−53.0	−0.4	2807	3000
15	0.067494	0.002114	0.281467	0.000026	−46.2	5.7	2572	2629
16	0.019503	0.000667	0.281314	0.000026	−51.6	2.7	2683	2813

Table 8 (*continued*)

Spot No.	$^{176}Yb/^{177}Hf$	$^{176}Lu/^{177}Hf$	$^{176}Hf/^{177}Hf$	Error ($2\sigma_m$)	$\varepsilon_{Hf}(0)$	$\varepsilon_{Hf}(t)$ (2.5Ga)	T_{DM1} (Ma)	T_{DM2} (Ma)
17	0.021445	0.000684	0.281243	0.000024	−54.1	0.1	2780	2970
18	0.005760	0.000190	0.281297	0.000022	−52.2	2.9	2673	2802
19	0.043441	0.001295	0.281378	0.000019	−49.3	3.9	2640	2739
20	0.112529	0.002961	0.281478	0.000026	−45.8	4.7	2616	2692
21	0.013961	0.000425	0.281312	0.000029	−51.6	3.0	2669	2793
22	0.005683	0.000202	0.281308	0.000026	−51.8	3.2	2660	2780
03ZT-15								
1	0.024326	0.000733	0.281342	0.000021	−50.6	4.5	2650	2735
2	0.009630	0.000346	0.281317	0.000068	−51.4	4.3	2656	2748
3	0.018493	0.000670	0.281375	0.000081	−49.4	5.8	2601	2656
4	0.020894	0.000740	0.281311	0.000089	−51.7	3.4	2692	2803
5	0.026618	0.001041	0.281368	0.000063	−49.7	4.9	2636	2711
6	0.018441	0.000689	0.281345	0.000068	−50.5	4.7	2643	2724
7	0.012565	0.000476	0.281301	0.000058	−52.0	3.5	2687	2797
8	0.006756	0.000319	0.281216	0.000078	−55.0	0.7	2790	2965
9	0.006001	0.000218	0.281244	0.000068	−54.1	1.9	2746	2895
10	0.012497	0.000422	0.281267	0.000065	−53.2	2.3	2729	2866
11	0.056406	0.001697	0.281432	0.000109	−47.4	6.0	2592	2639
12	0.010585	0.000422	0.281289	0.000059	−52.4	3.1	2700	2818
13	0.015666	0.000529	0.281279	0.000064	−52.8	2.6	2720	2850
14	0.025620	0.000903	0.281232	0.000062	−54.5	0.3	2811	2992
15	0.014323	0.000486	0.281274	0.000080	−53.0	2.5	2724	2857
16	0.012325	0.000414	0.281261	0.000059	−53.4	2.1	2736	2877
17	0.027627	0.000928	0.281354	0.000069	−50.2	4.6	2647	2729
18	0.015507	0.000527	0.281342	0.000072	−50.6	4.8	2635	2712
19	0.022019	0.000825	0.281326	0.000068	−51.1	3.8	2677	2779
20	0.016822	0.000563	0.281371	0.000078	−49.6	5.8	2599	2654

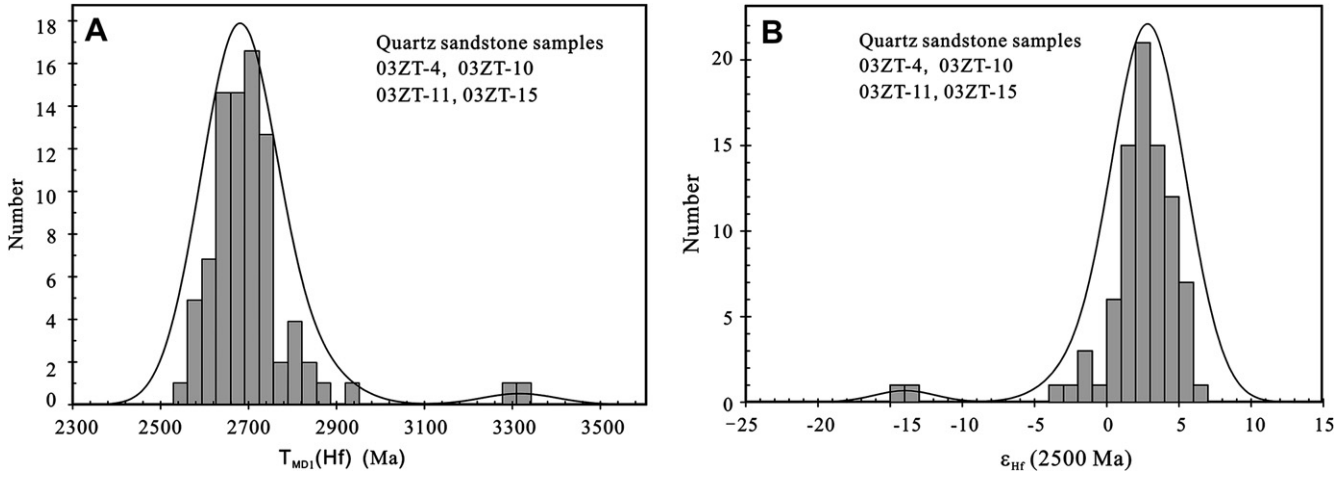

Fig. 10. (A) Frequency histogram of initial ε_{Hf} values of detrital zircon grains of sandstone samples 03ZT-4, 03ZT-10, 03ZT-11, and 03ZT-15, obtained using the LA-MC-ICP-MS method. Initial ε_{Hf} values, calculated back to 2500 Ma, cluster around +4. (B) Frequency histogram of T_{DM}(Hf) values of detrital zircon grains of sandstone samples 03ZT-4, 03ZT-10, 03ZT-11, and 03ZT-15, obtained using the LA-MC-ICP-MS method. T_{DM} (Hf) values calculated using crustal Lu/Hf ratios from Griffin et al., 2000), give an age peak around 2700 Ma.

Formation and mica quartz phyllites of the lower Aguluguo Formation, which were deposited above the intercalated volcanic rocks, have considerably higher initial ε_{Nd} values. This shift implies a significant change in the sedimentary source. It seems that the upper part of the Zhaertai Group was increasingly affected by mantle material or by the young (early Mesoproterozoic) magmatic rocks of mantle origin. The mafic dyke swarms of about 1780 Ma to 1750 Ma exposed in the North China Craton can be roughly divided into two groups according to their Nd isotopic composition (Wang et al., 2004; Peng, 2005; Peng et al., 2005). One group of mafic dykes has initial ε_{Nd} values commonly lower than about −3.0, similar to the basalts

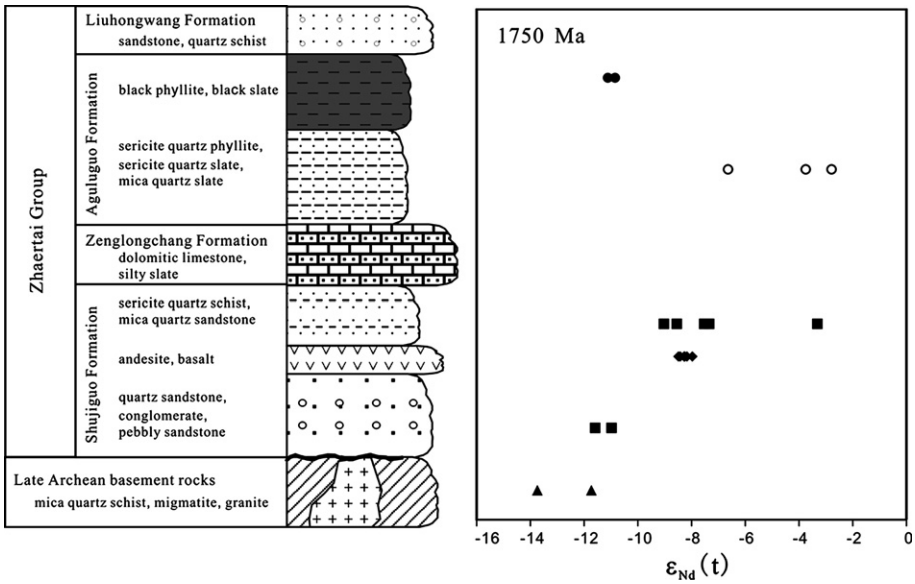

Fig. 11. Variation of initial ε_{Nd} values of whole-rock samples related to stratigraphic sequence. Initial ε_{Nd} values were calculated back to 1750 Ma (a mean sedimentation age of the Zhaertai Group).

of the Zhaertai Group, while another group exhibits higher ε_{Nd} values (>-2.0 and many of them >0). Mesoproterozoic mafic rocks of mantle origin possibly resulting from mantle upwelling subsequently provided material for the upper Zhaertai Group, causing higher initial ε_{Nd} values. Therefore, the early Mesoproterozoic event, related either to breakup of the supercontinent Columbia (e.g., Peng et al., 2005) or to post-collisional collapse of the Trans-North China orogen (e.g., Zhao et al., 2000, 2005; Wang et al., 2004), is a key for understanding the origin and evolution of Mesoproterozoic rifting in the North China Craton. Black phyllites of the upper Aguluguo Formation again yield lower initial ε_{Nd} values and have significantly higher Nd model ages (about 3.4 Ga) than other rock types of the Zhaertai Group, indicating a lack of contribution from juvenile material.

8. Conclusions

The intercalated mafic volcanic rocks in the lower part of the Zhaertai Group, dated at about 1743 Ma, have low initial ε_{Nd} values of −8.49 to −7.97, similar to the contemporaneous mafic dyke swarms within the North China Craton that are likely related to breakup of the supercontinent Columbia. Deposition of the Zhaertai Group likely started shortly before the formation of the volcanic rocks (about 1750 Ma). Sandstone samples collected from the lower part of the Zhaertai Group contain detrital zircon populations of about 2500 Ma that originated from late Archean basement rocks that are widely distributed in the North China Craton. No Paleoproterozoic detrial zircons have been detected in sandstones of the Zhaertai Group, probably implying that Paleoproterozoic magmatism was much weaker at the northern margin than the inner parts of the North China Craton or that the Paleoproterozoic basement rocks were not exposed at the surface.

The detrital zircon grains yield T_{DM1}(Hf) values clustering around 2700 Ma. Most of the sandstone samples also have positive initial ε_{Nd} values at 2500 Ma. This Hf and Nd isotopic feature implies a juvenile character for the late Archean basement protoliths. The ε_{Nd} values of whole rock samples collected from the Zhaertai Group increase progressively upwards in the stratigraphic sequence. This variation indicates a change in the sources of the sedimentary material. Late Archean basement rocks contributed sedimentary material at the beginning of the rifting at about 1750 Ma. Mesoproterozoic mafic rocks of mantle origin possibly resulting from mantle upwelling subsequently provided material, causing higher ε_{Nd} values of the sedimentary rocks in the middle part of the stratigraphic sequence, especially for those stratigraphically above the intercalated volcanic rocks. Further tectonic exhumation caused erosion and subsequent deposition of older basement rocks, forming black shales with lower ε_{Nd} values stratigraphically in the upper part of the Zhaertai Group.

Acknowledgements

This study was supported by the National Natural Science Foundation of China (NSFC project Nos. 40525007 and 40421202) and by the Ministry of Science and Technology of China (G1999075502). Sincere thanks are due to L.-Q. Zhang for guide in field work, and L.-W. Xie for help in Hf isotopic analysis. G.-C. Zhao and Y.-F. Zheng reviewed the manuscript and provided very useful comments and suggestions for the manuscript improvement.

References

Blichert-Toft, J., Albarede, F., 1998. The Lu–Hf geochemistry of chondrites and evolution of the mantle-crust system. Earth Planet. Sci. Lett. 148, 243–258.

Chen, J.-L., Wu, T.-S., 1997. The regional stratigraphy in North China. Wiley, Ny, 199pp in Chinese with English abstract.

Chen, F., Hegner, E., Todt, W., 2000. Zircon ages and Nd isotopic and chemical compositions of orthogenisses from the Black forest, Germany: evidence for a Cambrian magmatic arc. Int. J. Earth Sci. 88, 791–802.

Chen, F., Siebel, W., Satir, M., 2002. Zircon U–Pb and Pb-isotope fractionation during stepwise HF-acid leaching and geochronological implications. Chem. Geol. 191, 153–162.

Chen, F., Guo, J.-H., Jiang, L.-L., Siebel, W., Cong, B.-L., Satir, M., 2003. Provenance of the Beihuaiyang lower-grade metamorphic zone of the Dabie ultrahigh-pressure collisional orogen, China: evidence from zircon ages. J. Asian Earth Sci. 22, 343–352.

Chen, F., Li, Q.-L., Li, C.-F., Li, X.-H., Wang, X.-L., Wang, F., 2005. Prospect of high precision mass spectrometer in isotope geochemistry. Earth Sci. 30, 639–645 (in Chinese with English abstract).

Chen, F., Li, X.-H., Wang, X.-L., Li, Q.-L., Siebel, W., 2007. Nd–Hf isotopic composition and basement age of the Baoshan block in the Yunnan Tethyan belt, SW China: evidence from Early Paleozoic and Early Mesozoic granites. Int. J. Earth Sci., in press, doi: 10.1007/s00531-006-0146-y.

Chu, N.-C., Taylor, R.N., Chavagnac, V., Nesbitt, R.W., Boella, R.M., Milton, J.A., German, C., Bayon, G., Burton, M., 2002. Hf isotope ratio analysis using multi-collector inductively coupled plasma mass spectrometry: an evaluation of isobaric interference corrections. J. Anal. At. Spectrom. 17, 1567–1574.

Compston, W., Williams, I.S., Meyer, C., 1984. U–Pb geochronology of zircons from lunar breccia 73217 using a sensitive high mass-resolution ion microprobe. J. Geophys. Res. 89 Suppl., B525–B534.

DePaolo, D.J., Linn, A.M., Schubert, G., 1991. The continental crustal age distribution; methods of determining mantle separation ages from Sm–Nd isotopic data and application to the Southwestern United States. J. Geophys. Res. 96, B2071–B2088.

Griffin, W.L., Pearson, N.J., Belousova, E., Jackson, S.E., van Achterbergh, E., O'Reilly, S.Y., Shee, S.R., 2000. The Hf isotope composition of cratonic mantle: LAM-MC-ICPMS analysis of zircon megacrysts in kimberlites. Geochim. Cosmochim. Acta 64, 133–147.

Griffin, W.L., Wang, X., Jackson, S.E., Pearson, N.J., O'Reilly, S.Y., Xu, X., Zhou, X., 2002. Zircon chemistry and magma mixing, SE China: in-situ analysis of Hf isotopes, Tonglu and Pingtan igneous complexes. Lithos 61, 237–269.

Guo, J.-H., O'Brien, P.J., Zhai, M.-G., 2002. High-pressure granulites in the Sangan area, North China Craton: metamorphic evolution, P-T paths and geotectonic significance. J. Metamorph. Geol. 20, 741–756.

Halls, H.C., Li, J.-H., Davis, D., Hou, G.-T., Zhang, B.-X., Qian, X.-L., 2000. A precisely dated Proterozoic paleomagnetic pole form the North China Craton, and its relevance to paleocontinental construction: Geophys. J. Int. 143, 185–203.

Hanchar, J.M., Miller, C.F., 1993. Zircon zonation patterns as revealed by cathodoluminescence and backscattered electron images: implications for interpretation of complex crustal histories. Chem. Geol. 110, 1–13.

Huang, J.-Q., 1977. The basic outline of China tectonics. Acta Geol. Sinica 52, 117–135, in Chinese.

Jahn, B.M., Zhang, Z.Q., 1984. Archean granulite gneisses from eastern Hebei Province, China: rare earth geochemistry and tectonic implications. Contrib. Mineral. Petrol. 85, 224–243.

Kober, B., 1986. Whole-grain evaporation for $^{207}Pb/^{206}Pb$-age-investigations on single zircons using a double-filament thermal ion source. Contrib. Mineral. Petrol. 93, 482–490.

Kober, B., 1987. Single-Zircon evaporation combined with Pb^{+} emitter bedding for $^{207}Pb/^{206}Pb$-age investigations using thermal ion mass spectrometry, and implications to zirconology. Contrib. Mineral. Petrol. 96, 63–71.

Kröner, A., Compston, W., Zhang, G.-W., Guo, A.-L., Todt, W., 1988. Ages and tectonic setting of Late Archean greenstone – gneiss terrain in Henan Province, China, as revealed by single-grain zircon dating. Geology 16, 211–215.

Kröner, A., Wilde, S.A., Li, J.-H., Wang, K.-Y., 2005. Age and evolution of a late Archean to Paleoproterozoic upper to lower crustal section in the Wutaishan/Hengshan/Fuping terrain of northern China. J. Asian Earth Sci. 24, 577–595.

Kusky, T.M., Li, J.-H., 2003. Paleoproterozoic tectonic evolution of the North China craton. J. Asian Earth Sci. 22, 383–397.

Kusky, T.M., Li, J.-H., Tucker, R.D., 2001. The Archean Dongwanzi ophiolite complex, North China craton: 2.505-billion-year-old oceanic crust and mantle. Science 292, 1142–1145.

Li, J.-H., Kröner, A., Qian, X.-L., O'Brien, P., 2000. Tectonic evolution of an Early Precambrian high-pressure granulite belt in the North China craton. Acta Geol. Sinica 74, 246–258.

Li, J.-H., Kusky, T.M., Huang, X.-N., 2002. Archean podiform chromitites and mantle tectonics in ophiolitic mélange, North China craton: a record of early oceanic mantle processes. GSA Today 12, 4–11.

Liew, T.C., Hofmann, A.W., 1988. Precambrian crustal components, plutonic associations, plate environment of the Hercynian Fold Belt of central Europe: indications from a Nd and Sr isotopic study. Contrib. Mineral. Petrol. 98, 129–138.

Ludwig, K.R., 1988. Pbdat for MS-Dos – a computer program for IBM-PC compatibles for processing raw Pb–U–Th isotope data, US Geol. Surv., 1–37. Open-file Report, pp. 88–542.

Ludwig, K.R., 2001a. Isoplot/Ex, rev 2.49: A geochronological tookit for Microsoft Excel. Berkerley Geochron Center Spec. Publ. No. 1a, 58pp.

Ludwig, K.R., 2001b. Squid 1.02: a user manual. Berkerley Geochron. Center Spec. Publ. No. 2, 19pp.

Lu, S.-N., Yang, C.-L., Li, H.-K., Li, H.-M., 2002. A Group of rifting events in the terminal Paleoproterozoic in the North China Craton. Gondwana Res. 5, 123–131.

Ma, X.-Y., Bai, J., 1998. Precambrian crustal evolution of China. Springer Berlin-Heidelberg, Geol. Publ. House Beijing, pp. 331.

Machado, N., Simonetti, A., 2001. U–Pb dating and Hf isotopic composition of zircon by laser ablation MC-ICP-MS. In: Sylvester, P. (Ed.), Laser Ablation-ICPMS in the Earth Sciences: Principles and Applications, 29. Wiley, Canada, pp. 121–146.

Ma, X.-Y., Bai, J., Su, S.-T., Lao, Q.-Y., Zhang, J.-S., 1987. The early Precambrian geotectonic framework of China and study methods. Geol. Publ. House Beijing.

Mattauer, M., Matte, Ph., Malavieille, J., Tapponnier, P., Maluski, H., Xu, Z., Lu, Y., Tang, Y., 1985. Tectonics of the Qinling belt: build-up and evolution of eastern Asia. Nature 317, 496–500.

Meng, Q.-R., Zhang, G.-W., 2000. Geologic framework and tectonic evolution of the Qinling orogen, central China. Tectonophysics 323, 183–196.

Mezger, K., 1990. Geochronology in granulites. In: Vielzeuf, D., Vidal, Ph. (Eds.), Granulites and Crustal Evolution, 585. Kluwer Academic Publishers, pp. 451–470.

Nelson, D.R., 2001. An assessment of the determination of depositional ages for Precambrian clastic sedimentary rocks by U–Pb dating of detrital zircons. Sediment. Geol., 37–60.

Peng, P., 2005. Petrogenesis and tectonic significance of the ca. 1.8 Ga mafic dyke swarms in the central North China Craton. Dissertation, 213, in Chinese with English abstract.

Peng, P., Zhai, M.-G., Zhang, H.-F., Zhao, T.-P., Ni, Z.-Y., 2004. Geochemistry and geological significance of the 1.8 Ga mafic dike swarms in the North China craton: An example from the juncture of Shanxi, Hebei, and Inner Mongolia. Acta Petrol. Sinica 20, 439–456, in Chinese with English abstract.

Peng, P., Zhai, M.-G., Zhang, H.-F., Guo, J.-H., 2005. Geochronological constraints on the Paleoproterozoic evolution of the North China Craton: SHRIMP zircon ages of different types of mafic dikes. Int. Geol. Rev. 47, 492–508.

Pidgeon, R.T., Nemchin, A.A., Hitchen, G.J., 1998. Internal structures of zircons from Archaean granites from the Darling Range Batholith; implications for zircon stability and the interpretation of zircon U–Pb ages. Contrib. Mineral. Petrol. 132, 288–299.

Qian, X.-L., 1996. The nature of the early Precambian continental crust and its tectonic evolution model. Acta Petrol. Sinica 12, 169–178.

Rämä, O.T., Haapala, I., Vaasjoki, M., Yu, J.-H., Fu, H.-Q., 1995. 1700 Ma Shachang complex, northeast China : Proterozoic rapakivi granite not associated with Palaeoproterozoic orogenic crust. Geology 23, 815–818.

Roddick, J.C., Sullivan, R.W., Dudás, F.Ö., 1992. Precise calibration of Nd tracer isotopic composition for Sm–Nd studies. Chem. Geol. 97, 1–8.

Scherer, E.E., Cameron, K.L., Blichert-Toft, J., 2000. Lu–Hf garnet geochronology: closure temperature relative to the Sm–Nd system and the effects of trace mineral inclusions. Geochim. Cosmochim. Acta 64, 3413–3432.

Sengör, A.M.C., Natal'in, B.A., 1996. Paleotectonics of Asia: fragments of synthesis. In: Yin, A., Harrison, M. (Eds.), The Tectonic Evolution of Asia. Cambridge University Press, London, pp. 486–640.

Shao, J., Zhang, L.-Q., Guo, J.-H., Li, D.-M., 2001. Response of the north margin of the North China craton to breakup events of the global supercontinent in the Proterozoic. Gondwana Res. 4, 784–785.

Stacey, J.S., Kramers, J.D., 1975. Approximation of terrestrial lead isotope evolution by a two stage model. Earth Planet Sci. Lett. 26, 207–221.

Sun, S.S., 1982. Chemical composition and origin of the Earth's primitive mantle. Geochim. Cosmochim. Acta 46, 179–192.

Taylor, S.R., McLennan, S.M., 1985. The Continental Crust: Its Composition and Evolution. Blackwell, Oxford, 312pp.

Valverde, V.P., Dörr, W., Belka, Z., Franke, W., Wiszniewska, J., Schastok, J., 2000. U–Pb single-grain dating of detrital zircon in the Cambrian of central Poland; implications for Gondwana versus Baltica provenance studies: Earth Planet. Sci. Lett. 184, 225–240.

Wang, J., Li, S.-Q., Wang, B.-L., Li, J.-J., 1992. The Langshan – Baiyun Obo rift system. Series publications to the palte tectonics in the North China. Beijing University Press, Beijing, pp132 in Chinese with English abstract.

Wang, Y.-J., Fan, W.-M., Zhang, Y.-H., Guo, F., Zhang, H.-F., Peng, T.-P., 2004. Geochemical, $^{40}Ar/^{39}Ar$ geochronological and Sr–Nd isotopi constraints on the origin of Paleoproterozoic mafic dikes from the southern Taihang Mountains and implications for the ca. 1800 Ma event of the North China Craton. Precambrian Res. 135, 55–77.

Wiedenbeck, M., Allé, P., Corfu, F., Griffin, W.L., Meier, M., Oberli, F., von Quadt, A., Roddick, J.C., Spiegel, W., 1995. Three natural zircon standards for U–Th–Pb, Lu–Hf, trace element and REE analysis. Geostand. Newslett. 19, 1–23.

Wilde, S.A., Zhao, G.-C., Sun, M., 2002. Development of the North China Craton during the Late Archaean and its final amalgamation at 1.8 Ga: some speculation on its position within a global Paleoproterozoic supercontinent. Gondwana Res. 5, 85–94.

Wilde, S.A., Zhao, G.-C., Wang, K.-Y., Sun, M., 2004. First SHRIMP zircon U–Pb ages for Hutuo Group in Wutaishan: further evidence for Paleoproterozoic amalgamation of North China Craton. Chin. Sci. Bull. 19, 83–90.

Wilde, S.A., Cawood, P.A., Wang, K.-Y., Nemchin, A.A., 2005. Granitoid evolution in the Late Archean Wutai Complex, North China Craton. J. Asian Earth Sci. 24, 597–613.

Williams, I.S., 1998. U–Th–Pb geochronology by ion microprobe. In: McKibben, M.A., Shanks III, W.C., Ridley, W.I. (Eds.), Applications of Microanalytical Techniques to Understanding Mineralizing Processes. Rev. Econ. Geol. 7, pp. 1–35.

Woodhead, J., Hergt, J., Shelley, M., Eggins, S., Kemp, R., 2004. Zircon Hf-isotope analysis with an excimer laser, depth profiling, ablation of complex geometries, and concomitant age estimation. Chem. Geol. 209, 121–135.

Wu, C.-H., Zhang, C.-T., 1998. The Paleoproterozoic SW-NE collision model for the central North China Craton. Progress Precambrian Res. 21, 28–50.

Wu, R.-X., Zheng, Y.-F., Wu, Y.-B., Zhao, Z.-F., Zhang, S.-B., Liu, X.-M., Wu, F.-Y., 2006. Reworking of juvenile crust: element and isotope evidence from Neoproterozoic granodiorite in South China. Precambrian Res. 146, 179–212.

Xia, X., Sun, M., Zhao, G., Lou, Y., 2006a. LA-ICP-MS U–Pb geochronology of detrital zircons from the Jining Complex, North China Craton and its tectonic significance. Precambrian Res. 144, 199–212.

Xia, X., Sun, M., Zhao, G., Wu, F., Xu, P., Zhang, J., Lou, Y., 2006b. U–Pb and Hf isotopic study of detrital zircons from the Wulashan khondalites: Constraints on the evolution of the Ordos Terrane, western block of the North China Craton. Earth Planet. Sci. Lett. 241, 581–593.

Xu, P., Wu, F.-Y., Xie, L.-W., Yang, Y.-H., 2004. Hf isotopic compositions of the standard zircons for U–Pb dating. Chin. Sci. Bull. 49, 1642–1648.

Yang, Z.-Y., Cheng, Y.-Q., Wang, H.-Z., 1986. The geology of China. Oxford Monographs Geol. Geophys. 3, Oxford, pp303.

Yuan, H.-L., Gao, S., Liu, X.-M., Li., H.-M., Gunther, D., Wu, F.-Y., 2004. Accurate U–Pb age and trace element determinations of zircon by laser ablation-inductively coupled plasma mass spectrometry. Geostand. Newslett. 28, 353–370.

Zhai, M.-G., 2004a. 2.1–1.7 Ga geological event group and its geotectonic significance. Acta Petrol. Sinica 20, 1343–1354.

Zhai, M.-G., 2004b. Precambrian tectonic evolution of the North China Craton. In: Malpas, J., Fletcher, C.J.N., Ali, J.R., Aitchison, J.C. (Eds.), Aspects of the tectonic evolution of China. Geol. Soc. London, Spec. Publ. 226, pp. 57–72.

Zhai, M.-G., Liu, W.-J., 2003. Paleoproterozoic tectonic history of the North China craton: a review. Precambrian Res. 122, 183–199.

Zhai, M.-G., Bian, A.-G., Zhao, T.-P., 2000. The amalgamation of the supercontinent of the North China Craton at the end of Neo-Archean and its breakup during late Paleoproterozoic and Mesoproterozoic. Sci. China (D) 43, 219–232.

Zhang, F.-Q., Liu, J.-Z., Ouyang, Z.-Y., 1998. Tectonic framework of greenstone in the basement of the North China Craton. Acta Geophys. Sinica 41, 99–107.

Zhang, H.-T., So, C.-S., Yun, S.-T., 1999. Regional geologic setting and metallogenesis of central Inner Mongolia, China: guides for exploration of mesothermal gold deposits. Ore Geol. Rev. 14, 129–146.

Zhao, G.-C., Wilde, S.A., Cawood, P.A., Lu, L.Z., 1998. Thermal evolution of the Archean basement rocks from the eastern part of the North China Craton and its bearing on tectonic setting. Int. Geol. Rev. 40, 706–721.

Zhao, G.-C., Wilde, S.A., Cawood, P.A., Lu, L.Z., 1999. Tectonothermal history of the basement rocks in the western zone of the North China Craton and its tectonic implications. Tectonophysics 310, 223–240.

Zhao, G.-C., Cawood, P.A., Wilde, S.A., Sun, M., Lu, L.Z., 2000. Metamorphism of basement rocks in the Central Zone of the North China Craton: implications for Paleoproterozoic tectonic evolution. Precambrian Res. 103, 55–88.

Zhao, G.-C., Wilde, S.A., Cawood, P.A., Sun, M., 2001. Archean blocks and their boundaries in the North China Craton: lithological, geochemical, structural and P-T path constraints and tectonic evolution. Precambrian Res. 107, 45–73.

Zhao, G.-C., Cawood, P.A., Wilde, S.A., Sun, M., 2002. Review of global 2.1–1.8 Ga orogens: implications for a pre-Rodinia supercontinent. Earth-Sci. Rev. 59, 125–162.

Zhao, G.-C., Sun, M., Wilde, S.A., Li, S.-Z., 2003. Assembly, accretion and breakup of the Paleo-Msoproterozoic Columbia Supercontinent: records in the North China Craton. Gondwana Res. 6, 417–434.

Zhao, G.-C., Sun, M., Wilde, S.A., Li, S.-Z., 2005. Late Archean to Paleoproterozoic evolution of the North China Craton: key issues revisited. Precambrian Res. 136, 177–202.

Zheng, Y.-F., Zhao, Z.-F., Wu, Y.-B., Zhang, S.-B., Liu, X.-M., Wu, F.-Y., 2006. Zircon U–Pb age, Hf and O isotope constraints on protolith origin of ultrahigh-pressure eclogite and gneiss in the Dabie orogen. Chem. Geol. 211, 135–158.